

Pseudo-Triangulations — a Survey

Günter Rote, Francisco Santos, and Ileana Streinu

ABSTRACT. A pseudo-triangle is a simple polygon with three convex vertices, and a pseudo-triangulation is a tiling of a planar region into pseudo-triangles. Pseudo-triangulations appear as data structures in computational geometry, as planar bar-and-joint frameworks in rigidity theory and as projections of locally convex surfaces. This survey of current literature includes combinatorial properties and counting of special classes, rigidity theoretical results, representations as polytopes, straight-line drawings from abstract versions called combinatorial pseudo-triangulations, algorithms and applications of pseudo-triangulations.

CONTENTS

1. Introduction	1
2. Basic Properties of Pseudo-Triangulations	4
3. The Set of all Pseudo-Triangulations	14
4. 3D Liftings and Locally Convex Functions	20
5. Self-Stresses, Reciprocal Diagrams, and the Maxwell-Cremona Correspondence	29
6. Rigidity of Pseudo-Triangulations	33
7. All Generically Rigid Graphs are Pseudo-Triangulation Graphs	38
8. Polytopes of Pseudo-triangulations	47
9. Applications of Pseudo-Triangulations	53
References	62

1. Introduction

A *pseudo-triangle* is a simple polygon in the plane with exactly three convex vertices, called *corners*. A *pseudo-triangulation* is a tiling of a planar region

1991 *Mathematics Subject Classification.* Primary 05C62, 68U05; Secondary 52C25, 52B11.

Key words and phrases. computational geometry, triangulation, pseudo-triangulation, rigidity, polytope, planar graph.

First author partly supported by the Deutsche Forschungsgemeinschaft (DFG) under grant RO 2338/2-1.

Second author supported by grant MTM2005-08618-C02-02 of the Spanish Ministry of Education and Science.

Third author supported by NSF grants CCR-0430990 and NSF-DARPA CARGO-0310661.

into pseudo-triangles. In particular, a triangle is a pseudo-triangle and pseudo-triangulations are generalizations of triangulations. Special cases include the *pseudo-*

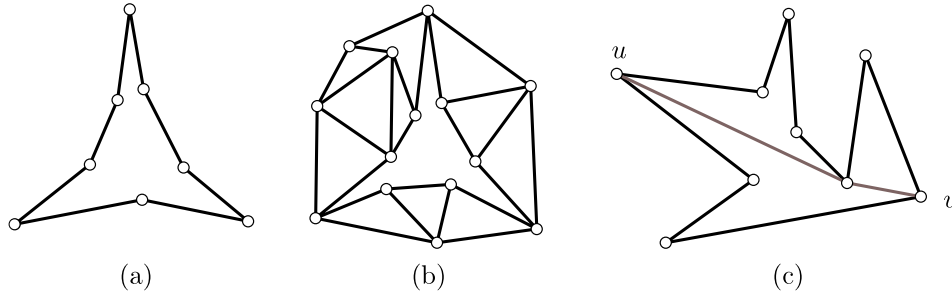


FIGURE 1. (a) A pseudo-triangle, (b) a pseudo-triangulation of a point set and (c) a pseudo-triangulation of a simple polygon, including a geodesic path from u to v .

triangulation of a finite point set and that of a *simple polygon*, which partition the convex hull of the point set, resp. the interior of the polygon, into pseudo-triangles and use no additional vertices. See Figure 1.

Pseudo-triangulations have arisen in the last decade as interesting geometric-combinatorial objects with connections and applications in visibility, rigidity theory and motion planning.

Historical perspective. The names *pseudo-triangle* and *pseudo-triangulation* were coined by Pocchiola and Vegter around 1995, inspired by a connection with pseudoline arrangements [39]. They were studying the *visibility complex* of a set of convex obstacles in the plane [40, 41], and defined pseudo-triangulations by taking a maximum number of non-crossing and free bitangents to pairs of objects, as in Fig. 2. For polygons, pseudo-triangulations had already appeared in the computational geometry literature in the early 1990's, under the name of *geodesic triangulations* [17, 22], and were obtained by tiling a polygon via non-crossing geodesic paths joining two polygon vertices, as in Figure 1(c). Compactness and ease of maintenance led to their use as efficient *kinetic data structures* for collision detection of polygonal obstacles [1, 12, 27, 26].

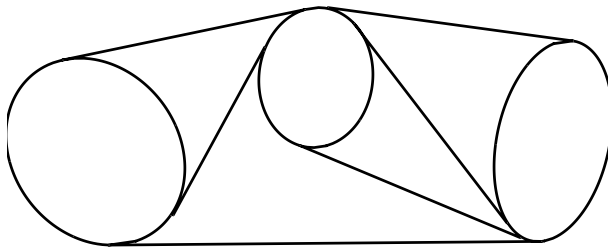


FIGURE 2. A pseudo-triangulation for three smooth convex obstacles.

In 2000, the work of Streinu [53] on the Carpenter's Rule Problem brought in an entirely different perspective from Rigidity Theory. She showed that *pointed*

pseudo-triangulations, when viewed as *bar-and-joint frameworks* (or *linkages with fixed edge-lengths*) are minimally rigid, and become expansive mechanisms with the removal of a convex hull edge. (A pseudo-triangulation is pointed if every vertex is incident to an angle larger than π , see Section 2 for more definitions.) Expansive motions were a crucial ingredient in the solution to the Carpenter’s Rule Problem by Connelly, Demaine and Rote earlier that year [19]. This newly discovered combinatorial expression was further exploited in [53] for a second, pseudo-triangulation-based, algorithmic solution of the same problem.

These results not only hinted for the first time to the deep connections between pseudo-triangulations and rigidity theory, but also highlighted their nice combinatorial properties and emphasized the importance of the concept of *pointedness*. They also led to the use of pseudo-triangulations in the investigation of the cone of all expansive infinitesimal motions of a point set [45], which resulted in the definition of the polytope of pointed pseudo-triangulations. This appears as a natural generalization of the well-studied associahedron [29], which corresponds to triangulations of a convex point set in the plane and thus, indirectly, to a long list of other combinatorial objects with ubiquitous applications in computer science and combinatorics (*Catalan structures* such as binary trees, lattice paths, stacks, etc.).

This work triggered several lines of research on pseudo-triangulations in the last five years. Here are most of those we are aware of:

- Two more *polytopes of pseudo-triangulations* have been found: one is a direct generalization of the polytope from [45] but covers all (not necessarily pointed) pseudo-triangulations [35]; the other is more an analogue of the *secondary polytope* of triangulations (see [15, 21]), and stems from the work of Aichholzer, Aurenhammer, Krasser, and Braß relating pseudo-triangulations to locally convex functions [5].
- There has been an increased interest in the study of combinatorial properties of pseudo-triangulations: their number, vertex degrees, and how these compare for different point sets or with respect to the analogous concepts in triangulations [7, 9, 6, 25, 42, 47].
- Related to this, but with algorithmic applications in mind, the *diameter* of the graphs of flips [4, 3, 13], and methods for the *efficient enumeration* of pseudo-triangulations [10, 14, 16] have been studied.
- The ultimate connection between planar graphs and pseudo-triangulations came with the proof that not only are pseudo-triangulations rigid (and pointed pseudo-triangulations minimally rigid), but the converse is also true: every planar (minimally) rigid graph admits a drawing as a (pointed) pseudo-triangulation [24, 36]. In order to prove this result, the concept of *combinatorial pseudo-triangulations* is introduced. They are defined as topologically embedded graphs in which the three *corners* of each pseudo-triangular face are specified.
- One of the key tools used in [19, 53] for the Carpenter’s Rule Problem was Maxwell’s Theorem from 1864, relating projections of polyhedral surfaces to plane self-stressed frameworks and to the existence of reciprocal diagrams. In the same spirit is the work of Aichholzer et al. [5], where a special type of locally convex piecewise-linear surface is related, via

projections, to pseudo-triangulations of polygonal domains. Maxwell’s reciprocal diagrams of (necessarily non-pointed) pseudo-triangulations are also considered in [34].

- As a further connection with rigidity theory, Streinu’s study of pointed pseudo-triangulations [53] was extended to *spherical pseudo-triangulations*, with applications to the spherical Carpenter’s Rule Problem and single-vertex origami [55]. This paper also contains partial work on combinatorial descriptions of expansive motions in three dimensions.
- In the theory of rigidity with fixed edge-directions (rather than fixed edge-lengths), pointed pseudo-triangulation mechanisms have been shown to have a kinetic behavior, linearly morphing tilings while remaining non-crossing and pointed [54].
- Finally, pseudo-triangulations have found applications as a tool for proofs: in the area of art galleries (illumination by floodlights) [51]; and in an area that is (at least apparently) unrelated to discrete geometry: to construct counter-examples to a conjecture of A. D. Alexandrov characterizing the sphere among all smooth surfaces [37].

Overview. This survey presents several points of view on pseudo-triangulations. First, as a tiling of a planar region, they are related to each other by local changes called flips. This is in several ways analogous to the ubiquitous triangulations which appear almost everywhere in Combinatorial Geometry, and has led to the investigation of similar questions: counting, enumeration, flip types, connectivity and diameter. We cover these topics in Sections 2 and 3. Next, in Section 4, we study their relationship with projections of locally convex surfaces in space. This serves as a bridge between the combinatorial and the rigidity properties of pseudo-triangulations, when viewed as bar-and-joint frameworks, which are presented in Sections 5, 6 and 7. Section 8 describes polytopes of pseudo-triangulations, whose construction relies on properties studied in the preceding Sections 4 and 6. Finally, in Section 9 we briefly sketch several applications of pseudo-triangulations that have appeared in the literature, a preview of which appears above in the historical introduction (ray shooting, visibility complexes, kinetic data structures, and Carpenter’s Rule problem).

The emphasis of this survey is on concepts and on the logical flow of ideas, and not so much on proofs or on the historical developments. But we sometimes have found shorter proofs than those on the literature, and we include those. In particular, in Section 4 we provide for the first time a uniform treatment for lifted surfaces in connection with pseudo-triangulations, which appeared independently in the context of the locally convex functions in [5], and in the rigidity-theory investigations of [53]. The results in Sections 3.4 and 7.5 are published here for the first time.

2. Basic Properties of Pseudo-Triangulations

Pseudo-triangulations generalize and inherit certain properties from triangulations. This section and the next one address their similarities in a comparative manner.

In this section, after fixing the basic terminology and notation to be used throughout, we exhibit the simple relationships that exist among several parameters of a pseudo-triangulation: numbers of vertices, edges, faces, pointed vertices,

convex hull or outer boundary vertices. They lie at the heart of the more advanced combinatorial properties presented later.

2.1. Definitions. A *graph* $G = (V, E)$ has n vertices, $V = \{1, \dots, n\}$ and $|E| = m$ edges. A *geometric graph* is a drawing of G in the plane with straight-line edges. The mapping $V \rightarrow \mathbb{R}^2$ of the vertices V to a set of points $P = \{p_1, \dots, p_n\}$ is referred to as the (straight-line) *drawing*, *embedding* or *realization* of G . With few exceptions, we will consider realizations on point sets with distinct elements (which induce edge segments of non-zero length), and in general position (which simplifies the analysis of *pointed* graph embeddings, defined below).

Plane graphs. A geometric graph G is *non-crossing* or *planar* if two disjoint edges $ij, kl \in E$, $(i, j \notin \{k, l\})$ are realized as disjoint (closed) line segments. The complement of the points and edges is a collection of planar regions called faces, one of which is unbounded. When G is connected, the bounded faces are topologically disks, and the unbounded face is a disk with a hole. A graph is *planar* if it has a planar embedding. With few exceptions, the graphs considered in this paper are planar and connected.

Polygons and corners. A simple polygon is a non-crossing embedding of a cycle. It partitions the plane into an interior region R and an exterior, unbounded one. More generally, we may encounter degenerate disk-like open polygonal *regions*, which have non-simple (self-touching but non-crossing) polygonal boundaries, called *contours*, as in Fig. 4 (right) on p. 9.

A vertex of a polygonal region (simple or degenerate) is called *convex*, *straight* or *reflex* depending on whether the angle spanned by its two incident edges, facing the polygonal region, is strictly smaller, equal to or strictly larger than π , respectively. General position for the vertices, which we usually assume, implies the absence of straight angles. Convex vertices incident to a face are also called *corners* of that face.

Pseudo- k -gons, pseudo-triangles. A simple polygon with exactly k corners is called a pseudo- k -gon. The special cases $k = 3$ and $k = 4$ are called *pseudo-triangles*, resp. *pseudo-quadrilaterals*. A bounded face must have at least 3 corners, but the unbounded face may be a pseudo- k -gon with $k \leq 2$.

Point sets, polygons and pointgons. We will work with point sets (denoted P), polygons (denoted R) and what we call *pointgons*. A *pointgon* (R, P) is a polygon R together with a specified finite set of points P consisting of all the vertices of R together with (perhaps) additional points in its interior. A polygon P is a special case of a pointgon, with no interior points. Similarly, a point set P can naturally be considered a pointgon, in which R is the convex hull of P .

Pointed graph embeddings. A vertex of an embedded graph is called *pointed* if some pair of consecutive edges (in the cyclic order around the vertex) span an angle larger than π , and *non-pointed* otherwise. The two edges incident to the reflex angle are called the *extreme* edges of the pointed vertex. A pointed (planar) graph embedding is one with all its vertices pointed.

Pseudo-triangulations. A pseudo-triangulation is a planar embedded connected graph whose interior faces are pseudo-triangles. The following three variants have been considered in the literature, depending on whether the boundary is allowed to be non-convex or whether interior points are allowed as vertices:

- A *pseudo-triangulation of a simple polygon* P is a subdivision of the interior of P into pseudo-triangles, using only vertices of P as vertices.

- A *pseudo-triangulation of a pointgon* (R, P) partitions the interior of the polygon P into pseudo-triangles using as vertices all of the points P .
- A *pseudo-triangulation of a finite point set* P is a pseudo-triangulation of the pointgon (R, P) , where R is the convex hull of P . In particular, a triangulation of P (using all vertices) is a pseudo-triangulation.

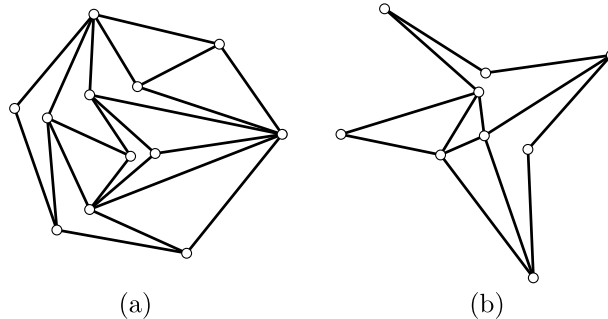


FIGURE 3. (a) a non-pointed pseudo-triangulation of a point set, (b) a non-pointed pseudo-triangulation of a pointgon.

In any of the variants, a *pointed pseudo-triangulation* is one in which every vertex is pointed. See Figure 1(b,c) for examples of pointed pseudo-triangulations, and Figure 3 for non-pointed ones.

2.2. Vertex and face counts. One of the basic properties of triangulations in the plane, which follows easily from Euler's Theorem, is that all triangulations of the same region and with the same set of vertices have the same number of edges (and of faces). The following theorem generalizes this to pseudo-triangulations.

Theorem 2.1. *Let (R, P) be a pointgon on $|P| = n$ points and r reflex vertices in the polygon R . Let T be a pseudo-triangulation of (R, P) with n_χ pointed vertices. Then T has $2n - 3 + (n_\chi - r)$ edges and $n - 2 + (n_\chi - r)$ pseudo-triangles.*

PROOF. Let m denote the number of edges. Then $2m$ equals the total number of angles in T , since a vertex of degree d is incident with d angles. Now we count separately the number of convex and reflex angles. The reflex angles are $n - n_\chi$ (one at each pointed vertex). The convex angles are the three in each pseudo-triangle plus the exterior angle of each reflex vertex of R . Hence,

$$2m = 3t + r + n - n_\chi,$$

where t is the number of pseudo-triangles. By Euler's Formula, $m + 1 = n + t$. Eliminating t (respectively m) from these two formulas gives the statement. \square

Here are some interesting special cases:

Triangulations. In this case the only pointed vertices are the convex vertices of R , so that $n_\chi = r + n_I$, where n_I is the number of interior vertices. This leads to the well-known relation $|E| = 2n - 3 + n_I$.

Pseudo-triangulations of a point set. The polygon R has only reflex exterior angles, so that $r = 0$. The number of pointed vertices can go from the number n_B of vertices of R in the case of a triangulation to n in the case of a pointed pseudo-triangulation.

Theorem 2.2. *Let P be a point set with n elements. Then, every pseudo-triangulation T of P has $2n - 3 + n_\chi$ edges, where n_χ is the number of non-pointed vertices in it.*

In particular, pointed pseudo-triangulations have the minimum possible number of edges, namely $2n - 3$, among all pseudo-triangulations of P . This motivated the term *minimum* pseudo-triangulations in [53], for what are now called pointed pseudo-triangulations.

Geodesic Pseudo-Triangulations. Pointed pseudo-triangulations of a simple polygon P are also called *geodesic triangulations*, because they arise by inserting a maximal number of non-crossing geodesic paths in P . The *geodesic path* between two points (typically, but not necessarily, two vertices) of a polygon R is the shortest path from one to the other *in R* (with R understood as a region). The geodesic path between two consecutive corners of a polygon is a sequence of polygon edges called a *pseudo-edge*. Figure 1c shows a geodesic path in a pseudo-5-gon, consisting of two edges. In general, a geodesic path between two *corners* will always consist of polygon edges and interior diagonals (where a *diagonal* is any segment joining two vertices of R through the interior of R). These particular diagonals are called interior *tangents*. Observe that a polygon is a pointed graph, and that geodesics between corners keep it pointed. In fact, this allows us to give a different definition of tangent diagonal: a diagonal e of a polygon R is called *tangent* if the graph $R \cup e$ is pointed.

A tangent may be part of several geodesics, but there is always a canonical one:

Lemma 2.3. *For every tangent of R there is a unique pair of corners such that the geodesic between them consists only of this tangent plus some (perhaps none) boundary edges of R .*

PROOF. Extend the tangent by following at each end, in the direction of tangency, a (possibly empty) sequence of edges into the next corner. \square

Geodesic triangulations have $n_\chi = 0$ and also $r = n - k$, where k is the number of corners. The number of edges in a pointed pseudo-triangulation of a pseudo- k -gon is therefore $n + k - 3$.

Theorem 2.4. *Every pointed pseudo-triangulation of a pseudo- k -gon consists of $k - 2$ pseudo-triangles and uses $k - 3$ interior tangents of R .*

2.3. Pointedness. Pseudo-triangulations may be regarded as maximal non-crossing graphs with a prescribed set of pointed vertices:

Theorem 2.5. *A non-crossing graph T is a pseudo-triangulation of its underlying point set P if and only if its edge set is maximal among the non-crossing embedded graphs with vertex set P and with the same set of pointed vertices as T .*

PROOF. *Only if:* since T is a pseudo-triangulation of P , any additional edge will go through the interior of a pseudo-triangle. But pseudo-triangles have no tangents, so this edge creates a non-pointed vertex.

If: suppose that no edge can be inserted without making some pointed vertex non-pointed. In particular, all convex hull edges of P are in T , are pointed and cannot be made non-pointed by the addition of any edge. We prove that every interior face R is a pseudo-triangle. A priori, the face may not even be simply connected if T is not connected, but it will always have a well-defined outer contour. Number the corners of R along this contour from v_1 to v_k , $k \geq 3$. Consider two

paths γ_+ and γ_- from vertex v_1 to v_3 through the interior of R , close to the contour of R and in opposite directions. Now *shorten* them continuously as much as possible, i. e., consider geodesic paths γ'_1 and γ'_2 homotopic to them. Adding these paths will maintain pointedness at all pointed vertices. The only possibility for these geodesic paths not to add any edges to T is that they coincide (hence R is simply connected) and go along the boundary of R (hence v_1 and v_3 are consecutive corners, and R is a pseudo-triangle).

A similar argument works for the outer face, if it is not a convex polygon. \square

In particular, pointed pseudo-triangulations can be reinterpreted as the maximal non-crossing *and pointed* graphs, in the same way as triangulations are the maximal non-crossing graphs. This leads to the following list of equivalent characterizations of pointed pseudo-triangulations. Another one, which shows how to incrementally build pointed pseudo-triangulations adding one vertex at a time, will appear in Theorem 2.12.

Theorem 2.6 (Characterization of pointed pseudo-triangulations [53]). *Let T be a graph embedded on a set P of n points. The following properties are equivalent.*

- (1) *T is a pseudo-triangulation of P with the **minimum** possible number of edges.*
- (2) *T is a **pointed** pseudo-triangulation of P .*
- (3) *T is a pseudo-triangulation of P with $m = 2n - 3$ edges (equivalently, with $f = n - 2$ faces).*
- (4) *T is **non-crossing, pointed** and has $2n - 3$ edges.*
- (5) *T is **pointed, non-crossing**, and **maximal** (among the pointed non-crossing graphs embedded on P).*

PROOF. The first three equivalences, and the implication (2) \Rightarrow (4), follow from Theorem 2.1. The equivalence (2) \Leftrightarrow (5) is Theorem 2.5. The implication (4) \Rightarrow (5) is a combination of both theorems: every non-crossing pointed graph can be completed to a maximal one, which is, by Theorem 2.5, a pointed pseudo-triangulation and has, by Theorem 2.1, $2n - 3$ edges. If that was already the number of edges we started with, then the original graph was already maximal. \square

Pseudo-triangulations and Laman graphs. A graph G is called a *Laman graph* if it has $2n - 3$ edges and every subset of $n' \geq 2$ vertices spans at most $2n' - 3$ edges. By Theorem 2.2 the graph of every pointed pseudo-triangulation satisfies the first property. By Theorem 2.5 it also satisfies the second, since every subgraph will itself be pointed. Hence:

Corollary 2.7 (Streinu [53]). *The underlying graphs of pointed pseudo-triangulations of a point set are Laman graphs.*

This property indicates the deep connections between pseudo-triangulations and rigidity, which will be developed in Section 6. The same arguments for arbitrary pseudo-triangulations lead to:

Corollary 2.8. *Let T be a pseudo-triangulation of n points, n_χ of them non-pointed. Then, T has $2n - 3 + n_\chi$ edges and for every subset of $n' \geq 2$ vertices, n'_χ of them non-pointed, the induced subgraph has at most $2n' - 3 + n'_\chi$ edges.*

Note that this *generalized Laman property* is not a property of the abstract graph, but of a geometric one, since we need to know which vertices are pointed.

For a non-crossing geometric graph, let us define the *excess of corners* \bar{k} as the number of convex angles minus three times the number of bounded faces. The name indicates the fact that every bounded face has at least three corners. The excess of corners is at least zero, with equality if and only if the graph is a pseudo-triangulation of a point set. The following statement is the most general form of the formula for the number of edges of a non-crossing graph in terms of pointedness.

Theorem 2.9. *A connected geometric graph with m edges, n vertices, n_χ of which are non-pointed and with excess of corners \bar{k} satisfies:*

$$m = 2n - 3 + (n_\chi - \bar{k}).$$

The assumption of connectivity can be removed if \bar{k} is defined additively on connected components, as the number of convex angles minus three times the number of *bounded face cycles*.

PROOF. Use the same counts as in Theorem 2.1. There are $2m$ angles, $n - n_\chi$ of them reflex and $3f + \bar{k}$ convex, where f is the number of bounded faces. Hence,

$$2m = 3f + \bar{k} + r + n - n_\chi.$$

Euler's Formula $m + 1 = n + f$ finishes the proof. \square

In particular, the difference $n_\chi - \bar{k}$ does not depend on the particular non-crossing embedding of a given planar graph G . In Section 7.5 we shall discuss how small the parameters n_χ and \bar{k} can be, for a given G (Theorem 7.14).

2.4. Flips in pseudo-triangulations. Let T be a pseudo-triangulation of a pointgon (R, P) and let e be an interior edge, common to two pseudo-triangles Δ_1 and Δ_2 . If e is removed from T the two pseudo-triangles become a single region Γ that we can regard as a (perhaps degenerate, see Figure 4) polygon.

Proposition 2.10. *This polygon Γ is:*

- a pseudo-quadrilateral if both endpoints of e preserve their pointedness with the removal; this happens when e is a tangent of Γ .
- a pseudo-triangle, otherwise. In this case, exactly one of the endpoints changes from non-pointed to pointed with the removal.

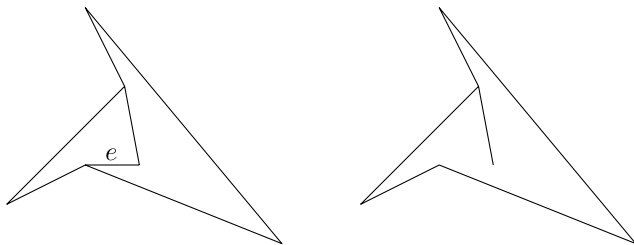


FIGURE 4. The removal of an edge may produce a degenerate pseudo-quadrilateral.

PROOF. The statement can be proved geometrically, by looking at the old and new angles at the endpoints of e . Here we offer a counting argument based on Theorem 2.9. Applied to T and to $T \setminus e$, the theorem gives

$$m = 2n - 3 + (n_X - \bar{k})$$

and

$$m - 1 = 2n - 3 + (n'_X - \bar{k}'),$$

where m , n , n_X and \bar{k} are the number of edges, vertices, non-pointed vertices and excess of corners in T , and n'_X and \bar{k}' are the same in $T \setminus e$. Hence,

$$n_X - \bar{k} = n'_X - \bar{k}' - 1.$$

If both endpoints keep their (non-)pointedness, then the excess of corners increases by one, which implies that Γ is a pseudo-quadrangle. If one endpoint passes from non-pointed to pointed then the excess of corners is preserved, and Γ is a pseudo-triangle. It is impossible for both endpoints to pass from non-pointed to pointed, since it would imply Γ being a pseudo-2-gon. \square

Since every pseudo-quadrilateral has exactly two pseudo-triangulations, obtained by inserting one or the other geodesic between opposite corners, we can define the following types of *flips* in a pseudo-triangulation T . See the examples in Figure 5.

- (*Diagonal flip*) If e is an interior edge whose removal does not produce a pseudo-triangulation, then there exists a unique edge e' different from e that can be added to obtain a new pseudo-triangulation: the other diagonal of the pseudo-quadrilateral Γ created in $T \setminus e$.
- (*Deletion flip*) The removal of an interior edge $e \in T$, if the result is a pseudo-triangulation.
- (*Insertion flip*) The insertion of a new edge $e \notin T$, if the result is a pseudo-triangulation.

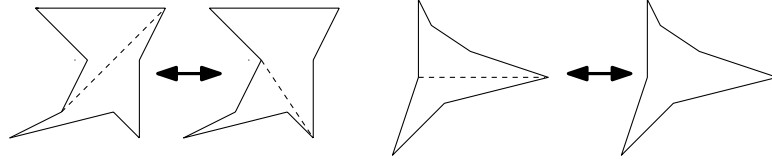


FIGURE 5. Left, a diagonal-flip. Right, an insertion-deletion flip.

The following result will be generalized in Theorem 2.13:

Proposition 2.11. *In every pseudo-triangulation T of (R, P) there is one flip for each interior edge and one for each pointed vertex that is not a corner of R .*

PROOF. By Proposition 2.10, we have exactly one deletion or diagonal flip on every interior edge, that deletes the edge and (if needed) inserts the other diagonal of the pseudo-quadrilateral formed.

An insertion flip is the inverse of a deletion flip and, by Proposition 2.10, it turns a pointed vertex p to non-pointed. Moreover, as long as the reflex angle at p is in a pseudo-triangle Δ (that is, if p is not a corner of R), there is one insertion flip possible at p , namely the insertion of the diagonal that is part of the geodesic from p to the opposite corner of Δ . \square

2.5. Henneberg constructions of pointed pseudo-triangulations. In pointed pseudo-triangulations, only the diagonal and insertion flips are possible. In particular, every interior edge can be flipped out to produce another pointed pseudo-triangulation. This implies that they can be incrementally constructed with the following procedure, called a *Henneberg construction* for historical reasons connected to the rigidity theoretic properties of pointed pseudo-triangulations:

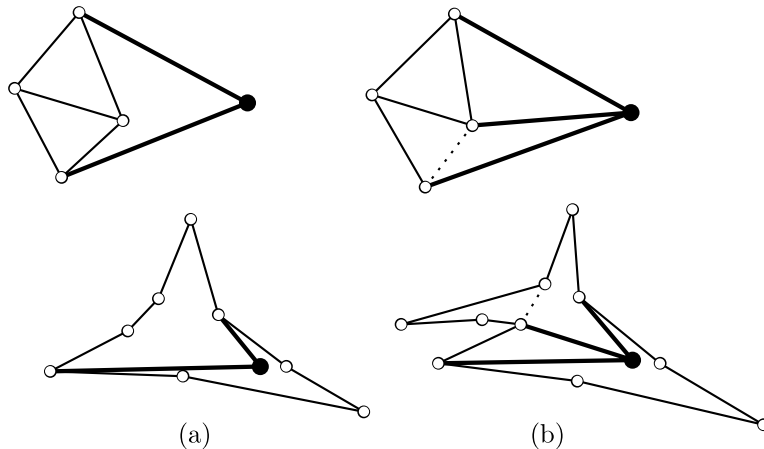


FIGURE 6. Henneberg steps. (a) type 1 and (b) type 2. Top row: the new vertex is added on the outside face. Bottom row: it is added inside a pseudo-triangular face. The added edges are thick. The dotted edge is the one that is removed in the type-2 step.

Theorem 2.12 (Streinu [53]). *Let T be a pointed pseudo-triangulation of a point set P . Then, there is an ordering p_1, p_2, \dots, p_n of the points in P and a sequence of pointed pseudo-triangulations T_i on the point set $\{p_1, \dots, p_i\}$ for $i = 3, \dots, n$ such that each T_{i+1} is obtained from T_i by one of the following two procedures (see Fig. 6):*

- (1) Type 1 (vertex of degree 2): *Join the vertex p_{i+1} by two segments. If p_{i+1} is in the outer face of T_i the segments are tangent to the boundary of T_i . Otherwise, the two segments are parts of geodesics to two of the three corners of the pseudo-triangle of T_i containing p_{i+1} .*
- (2) Type 2 (vertex of degree 3): *Add the vertex p_{i+1} with degree 2 as before, then flip an edge in the pseudo-edge opposite to p_{i+1} in the unique triangle that has p_{i+1} as a corner.*

PROOF. Since T has $2n - 3$ edges, the average degree of a vertex is $4 - 6/n$. In particular, there must be a vertex of degree two or three.

If there is a vertex of degree two, consider it the last vertex in the ordering, p_n . Removing the two edges incident to it leaves a pointed non-crossing graph on $n - 1$ vertices and with $2(n - 1) - 3$ edges, hence a pseudo-triangulation that we call T_{n-1} . Then, T is obtained from T_{n-1} by a type 1 step as described in the statement.

If there is no vertex of degree two, then there is a vertex of degree three, that we take as p_n . Since p_n is pointed, one of its edges lies within the convex angle

formed by the other two (and, in particular, it is an interior edge). Let T' be the pseudo-triangulation obtained by flipping that edge, in which p_n has degree two. Let T_{n-1} be the pseudo-triangulation obtained from T' by removing the two edges incident to p_n , as before. Then, T is obtained from T_{n-1} by a step of type 2, as described. \square

2.6. The Graph of Pseudo-Triangulations. The *graph of pseudo-triangulations* of a pointgon (R, P) has one node for each pseudo-triangulation of (R, P) and an arc joining T and T' if there is a flip producing one from the other. Since the inverse of every flip is again a flip, this is an undirected graph.

Theorem 2.13. *Let (R, P) be a pointgon with n vertices and n_I interior points.*

- (1) *Its graph of pseudo-triangulations is regular of degree $n + 2n_I - 3$.*
- (2) *The subgraph induced by pointed pseudo-triangulations is also regular, of degree $n - r + n_I - 3 = k + 2n_I - 3$, where r and k are the numbers of reflex vertices and corners in R .*

In both cases the graph is connected.

PROOF. By Proposition 2.11 the number of flips in a pseudo-triangulation equals the sum of its interior edges plus its pointed vertices other than corners of R . These two numbers are, respectively,

$$2n - 3 + (n_X - r) - n_B = n + n_I - 3 + (n_X - r)$$

and

$$n - n_X - k,$$

so its sum is

$$n + n_I - 3 + (n_X - r) + n - n_X - k = 2n + n_I - 3 - r - k = n + 2n_I - 3.$$

This proves part (1). For part (2), deletion flips do not happen and we are not interested in insertion flips. Hence, we only need to count interior edges, and also we have $n_X = 0$. Hence, the number of diagonal flips is:

$$2n - 3 - r - n_B = n - 3 - r + n_I.$$

We prove connectivity only in the case of pseudo-triangulations of a point set P . For pointgons, a proof can be found in [5]. Let p_i be a point on the convex hull of P . The crucial observation is that pseudo-triangulations of $P \setminus \{p_i\}$ (and flips between them) coincide with the pseudo-triangulations of P that have degree 2 at p_i , if in the latter we forget the two tangents from p_i to the convex hull of $P \setminus \{p_i\}$. By induction, we assume the pseudo-triangulations of $P \setminus \{p_i\}$ to be connected in the graph. On the other hand, in pseudo-triangulations with degree greater than 2 at p_i all interior edges incident to e can be flipped and produce pseudo-triangulations with smaller degree at e . \square

As an example, Figure 7 shows the graph of pseudo-triangulations of a set of five points, one of them interior. As predicted by Theorem 2.13, the whole graph is 4-regular and the graph of pointed pseudo-triangulations (the solid edges) is 3-regular. In the picture, both the solid and the whole graph are 1-skeletons of simple polytopes, of dimensions 3 and 4 respectively. That this happens for the graphs of pseudo-triangulations of arbitrary pointgons will be proved in Section 8 (Theorems 8.2 and 8.4). These polytopes generalize the well-known *associahedron*, whose 1-skeleton is the graph of flips in triangulations of a convex polygon.

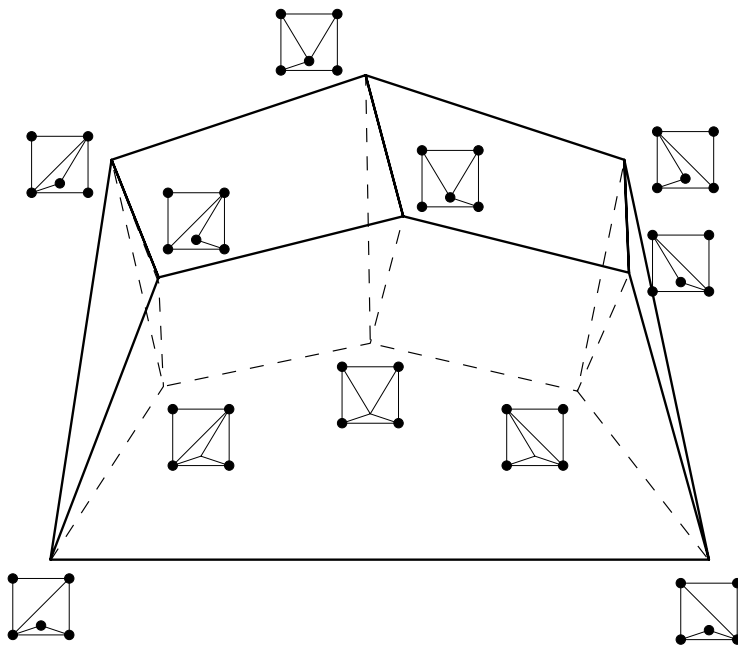


FIGURE 7. The graph of all pseudo-triangulations of this point set, connected by flips, forms the 1-skeleton of a 4-polytope. Pointed pseudo-triangulations form the 1-skeleton of a 3-polytope (solid lines)

Also of interest is the *diameter* of the graph of pseudo-triangulations, in other words, the number of flips that are necessary to go from one pseudo-triangulation to another:

Theorem 2.14. *For every set P of n points:*

- (1) (Bereg [13]) *The graph of all pseudo-triangulations of P has diameter bounded by $O(n \log n)$.*
- (2) (Aichholzer et al. [5]) *The subgraph induced by pointed pseudo-triangulations has diameter bounded by $O(n \log^2 n)$.*

The bounds are not known to be tight; no better bound than the trivial lower bound of $\Omega(n)$ is known. However, they are much better than the (worst-case) diameter of the graph of diagonal flips between triangulations of a point set, which can be quadratic as is well-known.

Observe that part (2) does not follow from part (1) since the distance between two pointed pseudo-triangulations can be increased when only pointed pseudo-triangulations are allowed as intermediate steps. An explicit example of this is shown in [3], where it is also shown that the diameter bound in part (1) can be refined to $O(n \log l)$ for a point set with l convex layers.

The graph of constrained pseudo-triangulations is also regular. By *constrained* one usually means that certain edges have to be used, but here we extend this notion to include also the fact that certain vertices are prescribed to be pointed. That is, let V be a subset of P containing no corners of R and let E be a set of

interior edges in (R, P) with the property that every $p \in V$ is pointed in E . We call *pseudo-triangulations of (R, P) constrained by E and V* all pseudo-triangulations whose graph contains E and whose pointed vertices contain V .

Theorem 2.15. *In the above conditions, let $c = |E| + |V|$. Then, the graph of pseudo-triangulations of (R, P) constrained by G and V is non-empty, connected, and regular of degree*

$$n + 2n_I - 3 - c.$$

This statement generalizes both parts of Theorem 2.13 ($c = 0$ and $c = n_I + r$, respectively).

PROOF. That the graph is not empty follows from Theorem 2.5. Regularity follows from part (1) of Theorem 2.13, since each constraint forbids exactly one flip. Connectedness can be proved with arguments similar to those in Theorem 2.13, and is also a consequence of Theorem 8.4. \square

3. The Set of all Pseudo-Triangulations

In this section we consider the set of all pseudo-triangulations of a given point set or pointgon and look at its structure *as a whole*.

3.1. Vertex and face degree bounds. Pseudo-triangles can have arbitrarily many edges. However, with a simple argument one can show that every point set has pointed pseudo-triangulations with bounded face-degree:

Theorem 3.1 (Kettner et al. [25]). *Every point set in general position has a pointed pseudo-triangulation consisting only of triangles and four-sided pseudo-triangles.*

PROOF. Triangulate the convex hull of P and then insert the interior points one by one via two edges each. It is easy to see that if p_i is a point in the interior of a triangle or four-sided pseudo-triangle Δ , then it is always possible to divide Δ into two triangles or four-sided pseudo-triangles by two edges incident to p_i . \square

More surprising is the result that the min-max vertex degree can also be bounded by a constant. Observe that for triangulations the situation is quite different: In *every* triangulation of the point set in Figure 9c in Section 3.3 below, the top vertex has degree $n - 1$.

Theorem 3.2 (Kettner et al. [25]). *Every point set P in general position has a pointed pseudo-triangulation whose maximum degree is at most five.*

The bound five cannot be improved.

It must also be noted that the method used in the following proof gives rise to an algorithm which, with appropriate data structures, runs in $O(n \log n)$ time.

PROOF. (Sketch) We construct the pointed pseudo-triangulation by successively refining a *partial pseudo-triangulation*, by which we mean a partition of the convex hull of P into some (empty) pseudo-triangles and some convex pointgons.

We start with the edges of the convex hull of the given point set, which defines a convex pointgon, as in Figure 8(a). At each subsequent step, one of the following two operations is used to subdivide one of the current convex pointgons (R', P') :

Partition. Choose a vertex p_i and an edge $p_j p_k$ of R' not incident to p_i . Choose also a line passing through p_i and crossing $p_i p_j$. If generic, this line splits P' into two subsets with p_i as their only common point. Then, subdivide R' into the convex hulls of these two subsets (two convex pointgons) plus the pseudo-triangle with corners p_i , p_j and p_k that gets formed in between. Except for the degenerate case described below, which produces only one pointgon, the degree of p_i increases by 2 and the degrees of p_j and p_k by one. See Figure 8(b).

Prune. A degenerate situation of partitioning arises when one of the two subsets consists only of p_i and one of p_j and p_k (say, p_j). (For this it is necessary, but not sufficient, that $p_i p_j$ is also a boundary edge of R'). The resulting partitioning produces a pseudo-triangle and only one new pointgon; the other one degenerates to a line segment and is ignored. The degrees of p_i and p_k increase by one. See Figure 8(c).

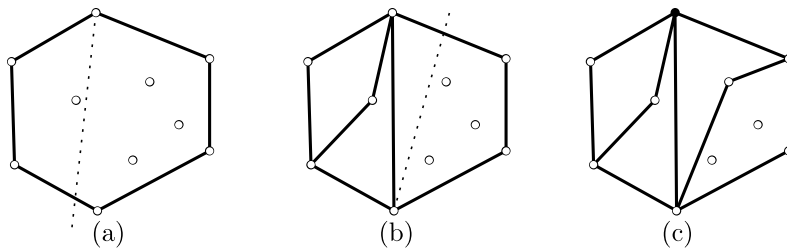


FIGURE 8. (a) Initial convex pointgon, (b) a *partition* step and (c) a *prune* step on the right convex pointgon from the previous step, pruning the black vertex on top.

Pruning and partitioning maintain both pointedness and planarity, and eventually they must lead to a pointed pseudo-triangulation. The rest of the proof consists in selecting these operations in the right order to satisfy some cleverly chosen invariants on the degrees of the boundary points of each convex subpolygon, and in this way guarantee that the degree does not exceed five.

To show that the bound five in the theorem cannot be reduced, Kettner et al. [25] proved that, for the vertex set of a regular $(2n + 1)$ -gon ($n \geq 5$) together with its center, every pointed pseudo-triangulation has some vertex of degree at least five. \square

3.2. Algorithms for Enumeration and Counting. In order to perform computer experiments that support or disprove statements, it is useful to have algorithms that *enumerate* all pseudo-triangulations of a given point set P explicitly. There are two algorithms for doing this in the literature. Both traverse an enumeration tree that is implicitly built on top of the graph of pointed pseudo-triangulations.

The algorithm of Bereg [14] is based on the reverse search paradigm of Avis and Fukuda [11]. It takes $O(n)$ space, and its running time is $O(\log n)$ times the number of pointed pseudo-triangulations.

Another enumeration algorithm has been given by Brönnimann, Kettner, Pocchiola, and Snoeyink [16]. They developed the *greedy flip* algorithm, which is based on an analogous algorithm by Pocchiola and Vegter [40] for the case of pseudo-triangulations of convex objects (cf. Figure 2). The enumeration tree that

the algorithm uses is a binary tree, and may contain “dead ends”, whose number can only be analyzed very crudely. The algorithm takes $O(n^2)$ space and the proved upper bound on the running time is $O(n \log n)$ times the number of pointed pseudo-triangulations. This algorithm has been implemented and, in practice, it seems to need only $O(\log n)$ time per pointed pseudo-triangulation. It can also be adapted to constrained pointed pseudo-triangulations, where a subset of the edges is held fixed.

The most stringent bottleneck to the applicability of these enumeration algorithms is not the time per pseudo-triangulation, but the exponential growth of the number of pointed pseudo-triangulations, see Section 3.3.

Other approaches to enumeration are conceivable. In particular the known enumeration algorithms for vertices of polytopes can be applied to the polytopes of pseudo-triangulations that are mentioned in Section 8. This would also lead to algorithms for enumerating all (pointed and non-pointed) pseudo-triangulations of a pointgon, or of pseudo-triangulations constrained in the sense of Theorem 2.15. These approaches have not been developed so far.

If one just wants to *count* pseudo-triangulations, it is not necessary to enumerate them one by one. A divide-and-conquer algorithm for counting (pointed or arbitrary) pseudo-triangulations is given by Aichholzer et al. [10]. A constraint set V of vertices which must be pointed can be specified.

3.3. The Number of Pseudo-Triangulations of a Point Set. What is the minimum and maximum number of pseudo-triangulations of a point set P , for a fixed cardinality n of P ? Before going on, let us summarize what is known about the analogous question for triangulations. We use the notations Θ^* , Ω^* and O^* to indicate that a polynomial factor has been neglected.

- For points in convex position, the number of triangulations (and of pseudo-triangulations) is the Catalan number $C_{n-2} = \frac{1}{n-1} \binom{2n-4}{n-2}$. Asymptotically, this grows as $\Theta(4^n n^{-3/2})$, or $\Theta^*(4^n)$.
- The number of triangulations of an arbitrary point set in general position is at most $O^*(43^n)$ [48] and at least $\Omega^*(2.33^n)$ [8]. Refined versions, for i interior and h convex hull points, are known: an upper bound of $O^*(43^i 7^h)$ from [48] and a lower bound of $\Omega(2.72^h 2.2^i)$ (or $\Omega(2.63^i)$, for fixed h) from [33].
- The point sets with the minimum and maximum number of triangulations known have asymptotically $\Theta^*(\sqrt{12}^n)$ and $\Theta^*(\sqrt{72}^n)$ triangulations.

The first one is the so-called *double circle*, consisting of a convex $n/2$ -gon and a point very close to the interior of every edge of it. The second one is a variation of the so-called *double chain*, consisting of two convex $n/2$ -gons *facing each other* so that each vertex of one of them sees all but one edges of the other. See these point sets in Figure 9.

The first difference with the case of pseudo-triangulations is that in pseudo-triangulations the minimum possible number is attained by points in convex position. This is still true if we only count *pointed* pseudo-triangulations:

Theorem 3.3 (Aichholzer et al. [6]). *Let P be a set of at least five points, at least one of them interior. Let p_0 be an interior point of P . Then, P has at least four times as many pointed pseudo-triangulations as $P \setminus \{p_0\}$. Moreover, every point set*

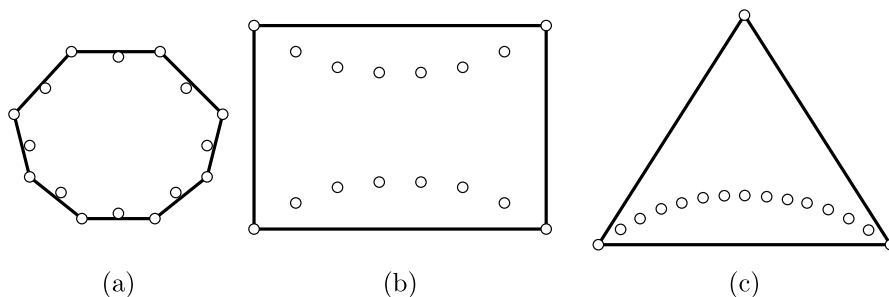


FIGURE 9. (a) A double circle; (b) a double chain; (c) a single chain, all with 16 points.

in general position has at least as many pointed pseudo-triangulations as the convex polygon with the same number of points.

PROOF (SKETCH). From each pointed pseudo-triangulation T of $P \setminus \{p_0\}$ we show how to construct (at least) four pointed pseudo-triangulations of P :

- (a) Three in which p_0 has degree two, obtained by a Henneberg step of type 1, as introduced in Theorem 2.12. That is, inserting two of the three geodesics that join p_0 to corners of the pseudo-triangle of T that contains p_0 in its interior.
- (b) One in which p_0 has degree three, obtained by a Henneberg step of type 2. That is, by performing a diagonal flip of an edge e opposite to p_0 in one of the pseudo-triangulations T' of the previous paragraph. The tricky part of the proof, which we omit, is to show that for at least one of the three choices of T' there is at least one choice of e that indeed increases the degree of p_0 from 2 to 3. Observe that, contrary to what happens in triangulations, a diagonal flip may not increase the degree of the opposite corners, since the diagonals of a pseudo-quadrilateral may not be incident to the corners (see the example in Figure 5).

We need to prove that this list contains no repetition. That is, that from the four pseudo-triangulations assigned to T we can actually recover T . For the three with degree two at p_0 this is obvious. For the fourth one, call it T'' it is also true: p_0 is pointed in T'' and has degree three, hence one of its edges is “between” the other two. T is recovered by first flipping this edge and then removing the two edges of p_0 that are left.

The last statement follows from the first part by induction on the number of interior points, using the fact that each Catalan number is smaller than four times the next Catalan number. In the only case where part (1) does not apply (four points, one of them interior) a direct check shows that the set has three pointed pseudo-triangulations, while the convex 4-gon has two. \square

It is convenient to stratify the set of pseudo-triangulations of a point set P according to the set of pointed vertices. For this, let V_B be the convex hull vertices of P and $V_I = V \setminus V_B$ be the set of interior points of P . Fix a subset $V_Y \subseteq V_I$, and let $PT(V_Y)$ be the set of pseudo-triangulations of V in which the points of V_Y are pointed and the remaining vertices $V_I \setminus V_Y$ are non-pointed. For example,

$PT(\emptyset)$ and $PT(V_I)$ are the triangulations and the pointed pseudo-triangulations of P , respectively.

Proposition 3.4 (Santos et al. [42]). *For every point set in general position, for any subset V_χ of interior points designated as pointed, and for every point $p_0 \in V_\chi$:*

$$|PT(V_\chi)| \leq 3 |PT(V_\chi \setminus \{p_0\})|$$

PROOF. Let us consider the graph of insertion/deletion flips that relate $PT(V_\chi)$ and $PT(V_\chi \setminus \{p_0\})$. This is a bipartite graph in which a pseudo-triangulation of $PT(V_\chi)$ is joined to the unique one obtained by the insertion flip that turns p_0 from pointed to non-pointed.

The statement follows from the claim that no pseudo-triangulation of $PT(V_\chi \setminus \{p_0\})$ has degree more than three in this graph. That is, that no more than three edges incident to any given vertex p_0 produce deletion flips that turn p_0 from non-pointed to pointed. This holds since for such an edge e , the two angles incident to e at p_0 must add to more than 180 degrees, and this cannot happen for more than three edges (in fact, it can only happen for two edges unless p_0 has degree three). \square

The previous statement says that the number of pseudo-triangulations *does not increase too much* if the prescription for a point changes from non-pointed to pointed. Experience and partial results show that the number actually *decreases*:

Conjecture 3.5. For every point set in general position, for any subset V_χ of interior points designated as pointed, and for every point $p_0 \in V_\chi$:

$$|PT(V_\chi)| \geq |PT(V_\chi \setminus \{p_0\})|$$

This conjecture is considered in [9], and proved to hold for three specific families of point sets: the double circle, the double chain, and the third point set of Figure 9. This set, called a “single-chain” consists of a convex $n - 1$ -gon together with a point that sees all of its edges except one. The asymptotic numbers of pseudo-triangulations of these point sets are also computed in [9], and summarized in the following table.

	double circle	double chain	single chain
triangulations	$\Theta^*(\sqrt{12}^n)$	$\Theta^*(8^n)$	$\Theta^*(4^n)$
pointed pseudo-triangulations	$\Theta^*(\sqrt{28}^n)$	$\Theta^*(12^n)$	$\Theta^*(8^n)$
all pseudo-triangulations	$\Theta^*(\sqrt{40}^n)$	$\Theta^*(20^n)$	$\Theta^*(12^n)$
Conjecture 3.5 holds?	YES	YES	YES

The number of triangulations of the single chain is just a Catalan number. It may come as a surprise that the double circle, which has as few triangulations as known so far, still has much more pointed pseudo-triangulations than the single chain, or the convex n -gon. But this is a consequence of Theorem 3.3.

To finish this section, as a joint application of Theorem 3.3 and Proposition 3.4 we obtain the following lower bound on the size of $PT(V_\chi)$:

Corollary 3.6. *For a point set with h points on the convex hull and i in the interior, and for every set V_χ of $k = |V_\chi|$ interior points designated to be pointed:*

$$PT(V_\chi) \geq \frac{PT(V_I)}{3^{i-k}} \geq \frac{C_{h+i-2}}{3^{i-k}} = \Theta^*(4^h (4/3)^i 3^k).$$

In particular, the total number of pseudo-triangulations is at least $\Omega^*(4^h(16/3)^i)$.

PROOF. The first inequality comes from applying Proposition 3.4 one by one to the non-pointed vertices in $V_I \setminus V_Y$. The second inequality is Theorem 3.3. The total number of pseudo-triangulations equals

$$\sum_{V_Y \subseteq V_I} PT(V_Y) \geq \sum_{V_Y \subseteq V_I} \frac{C_{h+i-2}}{3^{i-|V_Y|}} = \frac{C_{h+i-2}}{3^i} \sum_{V_Y \subseteq V_I} 3^{|V_Y|} = \frac{C_{h+i-2}}{3^i} 4^i. \quad \square$$

3.4. The number of geodesic triangulations of a polygon. The largest and smallest possible number of geodesic (pointed) pseudo-triangulations of a polygon with k corners is quite easy to obtain:

Theorem 3.7. *A pseudo- k -gon has between 2^{k-3} and C_{k-2} (the Catalan number) geodesic triangulations. Both bounds are achieved.*

PROOF. The upper bound is achieved by a convex k -gon. The lower bound is achieved by the pseudo- k -gon of Figure 10 whose diagonals come in $k-3$ crossing pairs. Every choice of one diagonal from each pair gives a geodesic triangulation.

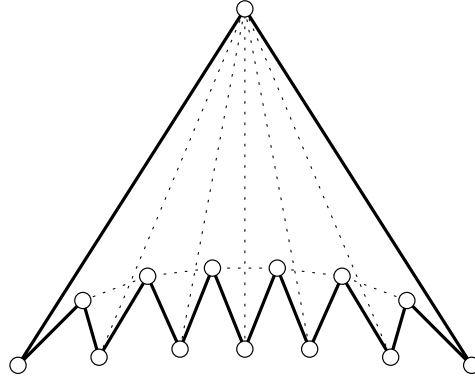


FIGURE 10. A pseudo- k -gon with 2^{k-3} pseudo-triangulations.

To prove the lower bound, let e be a diagonal in R . The diagonal e divides R into two polygons R' and R'' with k' and k'' corners respectively, with $k' + k'' = k + 2$. Then, the number of pointed pseudo-triangulations of R that contain this diagonal equals the product of the numbers of pointed pseudo-triangulations of R' and R'' . By inductive hypothesis this gives at least

$$2^{k'-3} \cdot 2^{k''-3} = 2^{k-4}$$

pointed pseudo-triangulations. But the number of geodesic triangulations that do not use e is at least the same number: to each pseudo-triangulation T that uses e we associate the one obtained by the flip at e , and no two choices of T produce the same T' , by Lemma 3.8 below.

For the upper bound, consider the k corners of R corresponding cyclically to the k vertices of a convex k -gon. To every triangulation \hat{T} of the k -gon we associate the geodesic triangulation T that uses the same geodesics. (This correspondence will be important again in Section 9.3, see Figure 31). That every pseudo-triangulation T of R arises in this way can be proved using Lemma 2.3: To each tangent of T we

associate its canonical geodesic, and consider the corresponding set of diagonals in the k -gon. These diagonals are mutually non-crossing, hence there is a triangulation \hat{T} containing all of them. \square

Lemma 3.8. *Let T be a pseudo-triangulation of a pointgon (R, P) and e a possible edge that is not used in T . Then, there is at most one diagonal flip in T that inserts e , unless one of the end-points of e is an interior vertex of degree two in T , in which case there may be two.*

PROOF. If an edge of T crosses e , then only the flip on that edge can insert e . If no edge of T crosses e , then e lies within a certain pseudo-triangle Δ of T . We regard the diagonal flip as obtained by first inserting e and then deleting another edge. (We do not need the intermediate graph to be a pseudo-triangulation, although it follows from our proof that indeed it is.)

Since a pseudo-triangle has no bitangent, e is not tangent to Δ at (at least) one of its end-points. On the other hand, if e can be inserted by a diagonal flip, e must be tangent to Δ at one of the ends, because otherwise the insertion of e turns both end-points from pointed to non-pointed and it will be impossible to make them both pointed again by the removal of a single edge. Hence, e is tangent to Δ at exactly one of its end-points. The other one, let us call it p_0 , is a reflex vertex of Δ . The edge removed by the flip must be one of its extremal edges, e_1 and e_2 . We now have two cases:

- (1) If p_0 has degree two in T then any of the two edges incident to it produces a flip that inserts e .
- (2) If there is another edge e' incident to p_0 in T besides e_1 and e_2 , then only the flip at the e_i that lies in the reflex angle formed by e and e' can possibly insert e by a diagonal edge, since e , e' and that e_i make p_0 non-pointed. \square

This lemma also shows that every pseudo- k -gon has at least $2(k-3)$ diagonals: the $k-3$ forming a geodesic triangulation plus the $k-3$ different (by the lemma) ones inserted by flips in it. So, the pseudo- k -gon of Figure 10 is also minimal in this sense.

Concerning possibly non-pointed pseudo-triangulations of a polygon, the analogue of Proposition 3.4 is true, with a similar proof but a better constant:

Proposition 3.9. *For every polygon, for any subset V_\times of reflex vertices of it designated as pointed, and for every point $p_0 \in V_\times$:*

$$|PT(V_\times)| \leq 2|PT(V_\times \setminus \{p_0\})| \quad \square$$

4. 3D Liftings and Locally Convex Functions

We switch now to a three-dimensional geometric problem which leads naturally to pseudo-triangulations of pointgons: locally convex polyhedral surfaces. This section is heavily based on Sections 3–5 of Aichholzer et al. [5], but some of the proofs are new. Specially, that of Lemma 4.10 is more direct than the original one.

4.1. The Lower (Locally) Convex Hull. Suppose a set of data points $p_i = (x_i, y_i)$ in the plane with associated height values h_i is given, and we look for the *highest* convex function $f: \mathbb{R}^2 \rightarrow \mathbb{R}$ that remains below the given height values:

$$(1) \quad f(x_i, y_i) \leq h_i, \text{ for all } i$$

Then it is well-known that the function f will be piecewise linear. It is defined on the convex hull of the point set P , and its graph is the lower convex hull of the points $(x_i, y_i, h_i) \in \mathbb{R}^3$, i. e., the part of the convex hull that is seen from below. If the height are sufficiently generic, the pieces where f is linear are triangles, forming a triangulation of a subset of P . (The resulting triangulations are called *regular triangulations* of P [21, 15, 20].)

We can ask the same question for a function f that is defined over a non-convex region polygonal R . But, now, it is natural to replace the condition of convexity by local convexity. A function $R \rightarrow \mathbb{R}$ is called *locally convex* if it is convex on every straight segment contained in R : For a pointgon (R, P) with given heights h_i at the points $p_i \in P$, we look for the *lower locally convex hull*, the (graph of the) highest function $f: R \rightarrow \mathbb{R}$ that fulfills (1). As shown by Aichholzer et al. [5], the regions on which f is linear form a pseudo-triangulation of a subset of P (Theorem 4.12).

Thus, pseudo-triangulations arise very naturally in this context: we start with a pointgon and some height values and construct the lower locally convex hull. The edges of this hull, when projected to the plane, yield a pseudo-triangulation.

4.2. Liftings of Plane Graphs. To study the problem of the lower locally convex hull, we will proceed in the opposite direction: we take a fixed pseudo-triangulation T in the plane and ask for the piecewise linear surfaces that project onto it (liftings of T). Along the way we get a simple but fundamental result that describes explicitly the space of liftings of a given pseudo-triangulation (Theorem 4.4). These results are relevant also for the rigidity properties of pseudotriangulations in Section 6.

Definition 4.1. Let G be a plane straight-line graph and let R be a union of (closed) faces of G . A (3D) *lifting* of (G, R) is the graph of a continuous function $f: R \rightarrow \mathbb{R}$ that restricts to an affine-linear function on each face of G , see Figure 11a. In other words, every face of G is lifted to a planar face in space.

As an important special case we have liftings of the whole plane $R = \mathbb{R}^2$. In this case, we usually insist that f is identically zero on the outer face, which can always be done by subtracting to a given f the affine-linear function it coincides with in the outer face. By the Maxwell-Cremona theorem (see Theorem 5.1), these 3D liftings have correspondences to other objects: reciprocal diagrams, which are treated in Section 5.2, and self-stresses, which are treated in Section 5.1.

On the other hand, when G is a pseudo-triangulation of a pointgon (R, P) , we don't care about the outer face, and we consider f defined only on the domain $R \subset \mathbb{R}^2$. In this case, the boundary vertices need not be coplanar in the lifting. We will not distinguish between f as a function and the lifting as a three-dimensional surface (the graph of the function).

The following easy observation lies at the heart of many proofs that use liftings to prove properties of pseudo-triangulations, and it highlights the role of pointedness.

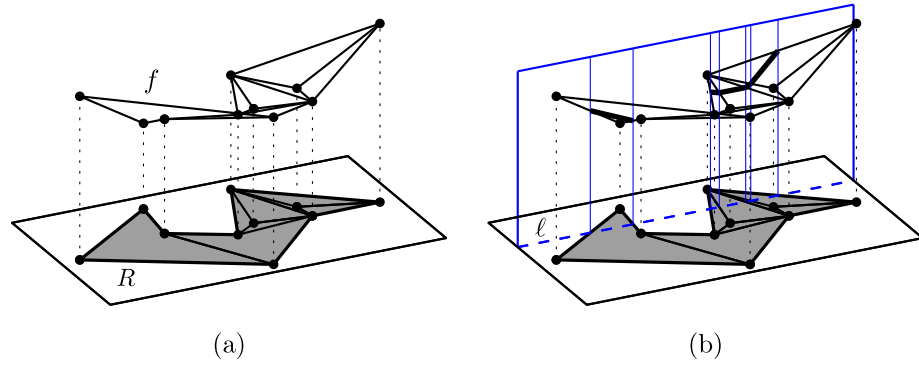


FIGURE 11. (a) A 3D lifting f of a geometric graph (in this case, a pseudo-triangulation) over a plane region R . (b) This lifting is locally convex. Looking at the restriction of f to a line ℓ , one sees that f cannot be extended to a convex function over \mathbb{R}^2 .

Lemma 4.2. *Let f be a lifting of a plane graph G over a region R . Let p be a vertex of G that is incident to a reflex vertex of some face $F \subset R$. If f has a global maximum at p , then f is constant on F , (and every point of the interior of F is a maximum point of f).*

PROOF. On any segment through p contained in F , f is linear, and hence must be constant if p is a maximum, see Figure 12. By considering two non-parallel segments through p , we conclude that f is constant on F . \square

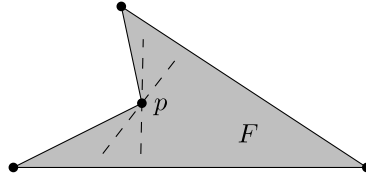


FIGURE 12. The lifting must be horizontal on every segment in F passing through p .

A vertex p as in the lemma is necessarily pointed, but a pointed vertex on the boundary of R does not always satisfy the condition of the lemma. This motivates the following classification. We call a vertex p *pointed in R* , or *relative pointed*, if it is a reflex vertex of some (and then a unique) region of G contained in R . Otherwise it is called *relative nonpointed*. (This corresponds to the classification into “incomplete” and “complete” vertices in [5].)

If one walks across a lifted edge between two faces, the slope may increase, decrease, or remain the same. Accordingly, we call the lifted edge a *valley edge*, a *mountain edge* (or *ridge*), or a *flat edge*. At valley and mountain edges, the function f is (locally) convex and concave, respectively.

Lemma 4.3. *The maximum and minimum height in every lifting is attained at some relative nonpointed vertex.*

PROOF. We take a convex hull vertex p of the set of vertices where the maximum height is attained. It follows from Lemma 4.2 that p cannot be a relative pointed vertex. \square

4.3. Liftings of Pseudo-Triangulations. Let T be a fixed pseudo-triangulation of a pointgon (R, P) .

Clearly, the liftings of T form a vector space that can be considered a subspace of the space \mathbb{R}^P of all maps $P \rightarrow \mathbb{R}$. The constraints for the heights of the vertices of T to define a lifting are linear equalities: for each relative pointed vertex p_l , there is a linear equation specifying that the lifting of p_l lies in the plane containing the three lifted corners p_i, p_j, p_k of the unique pseudo-triangle in which p_l is reflex. More precisely, since p_l lies in the convex hull of p_i, p_j, p_k , there are unique coefficients $\lambda_i, \lambda_j, \lambda_k$ with $p_l = \lambda_i p_i + \lambda_j p_j + \lambda_k p_k$, with $\lambda_i + \lambda_j + \lambda_k = 1$ and $0 < \lambda_i, \lambda_j, \lambda_k < 1$. Then the equation for the heights z is

$$(2) \quad z_l = \lambda_i z_i + \lambda_j z_j + \lambda_k z_k$$

This equation is the algebraic reason behind the geometric proof of Lemma 4.2: z_l is a convex combination of the heights z_i, z_j, z_k of the three corners of the pseudo-triangle in which p_l is reflex.

The following result provides an explicit basis of the vector space of liftings, hence it shows what its dimension is. We offer a geometric proof of this result, different from the more algebraic proof in [5].

Theorem 4.4 (The Surface Theorem, Aichholzer et al. [5]). *Let T be a pseudo-triangulation of a pointgon (R, P) .*

- (i) *For every choice of heights for the relative nonpointed vertices of T , there is a unique lifting of T .*
- (ii) *The height of every relative pointed vertex is a linear function of the height of the relative nonpointed vertices, with nonnegative coefficients.*

PROOF. We use induction on the number of relative pointed vertices. If this number is zero, then every pseudo-triangle of T is a triangle and the statement is obvious. Otherwise choose a relative pointed vertex p of T . Let Δ be the pseudo-triangle of which p is a reflex vertex and let T' be the pseudo-triangulation obtained by the edge-inserting flip at p . The relative nonpointed vertices of T' are those of T plus p itself. Hence, by the inductive hypothesis, for every choice of height at this new vertex there is a unique lifting of T' . Moreover, the heights of relative pointed vertices depend linearly on this choice, and the maximum and minimum heights are always attained at some relative nonpointed vertices.

We keep the heights of the original relative nonpointed vertices of T fixed and vary the height of p . When the height chosen for p is very high, p is the global maximum of the lifting. In particular, it is above the plane that contains the three lifted corners of Δ . Similarly, when the height of p is very low, p is below that plane. Linearity implies that there is a unique height for p that makes p and the corners of Δ coplanar. This proves part (i). The linear dependence of the heights of relative pointed vertices on the given heights follows from the fact that the space of liftings is a linear space.

To prove monotonicity in part (ii), a similar argument works. If the dependence were not monotone, there would be a set of initial heights for the relative nonpointed vertices of T such that an increase in one of them (p) makes some relative pointed

vertex q go down. By linearity, this process can be extrapolated, and a large increase in the height of p would make the relative pointed vertex q go below every relative nonpointed vertex, a contradiction to Lemma 4.3. \square

Corollary 4.5. *Let T be a pseudo-triangulation of a pointgon (R, P) . Then, the linear space of its lifts has dimension equal to the number of relative nonpointed vertices.*

Remark 4.6 (“Non-projective” pseudo-triangulations). As a particular case of Theorem 4.4 we recover the familiar fact that if T is a triangulation (i.e., all vertices are relative nonpointed), then every choice of heights for the vertices induces a lift of T . But the, also familiar, fact that *sufficiently generic* choices of heights produce lifts in which no two adjacent faces are coplanar does not hold for pseudo-triangulations.

Consider, for example, a pseudo-triangulation T of (R, P) which contains a subset of interior pointed vertices such that: (1) the graph T' obtained by removing these interior vertices and their incident edges is still a pseudo-triangulation (of a different pointgon (R, P') , where $P' \subset P$), and (2) every relative nonpointed vertex of T is still relative nonpointed in T' . An example is shown in Figure 13a, in which T' is obtained by removing the three interior vertices and the dashed edges. In the terminology of [5], such a T is not “face-honest”. Theorem 4.4 implies that, when this happens, T and T' have exactly the same lifts. In particular, in every lift of T the faces of T that form a single face in T' are coplanar.

Theorem 5.4 in [5] is an attempt to characterize *projective* pseudo-triangulations; that is, those that admit lifts with no coplanar adjacent faces. Besides showing that projective pseudo-triangulations must be face-honest in the above sense, the authors give an example in which a face-honest pseudo-triangulation *in special position* is not projective (Figure 13b). But they also make the statement that if the vertex set P is sufficiently generic then every face-honest pseudo-triangulation of (R, P) is projective. This statement is, unfortunately, wrong, as Figure 13c shows. So, it remains an open question to characterize projective pseudo-triangulations, even for generic positions of the vertex set.

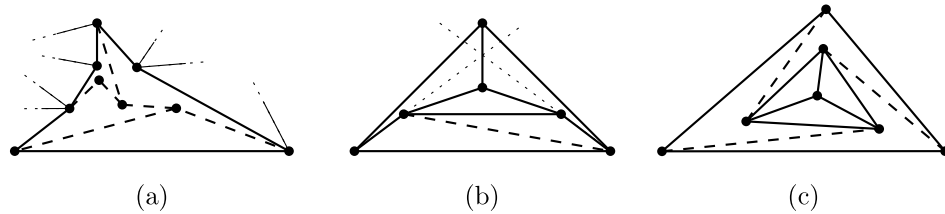


FIGURE 13. Some “non-projective” pseudo-triangulations, that can only be lifted with flat edges (shown dashed). (a) A pointed pseudo-triangulation inside a pseudotriangular face (which might form part of a larger graph) will always be lifted flat. (b) In this special position, the dashed edge is flat in any lifting. Perturbing the vertices will make the edge folded. (c) Even in generic vertex positions, the dashed edges are always lifted flat.

A common trick that has also been used in the last proof is that we vary the height of a single relative nonpointed vertex, keeping the other heights fixed. The following lemma describes the situation when this vertex is very high.

Lemma 4.7. *If, in some lifting, the relative nonpointed vertex p_i is higher than all other relative nonpointed vertices, then it is the unique global maximum in the lifting.*

PROOF. As in the proof of Lemma 4.3, we look at the convex hull of the set where the maximum height is attained. Every vertex of this convex hull must be a relative nonpointed vertex p_j , at its original height h_j . This vertex can only be p_i . \square

The previous lemma can be rephrased as “if the global maximum of a lifting is unique, then it is a relative nonpointed vertex. The following crucial local argument lies at the heart of its and other proofs.

Lemma 4.8. *Let p_i be a strict local maximum in some lifting $f: R \rightarrow \mathbb{R}$. Suppose that p_i is not a corner of R . Then, for every open half-plane H with p_i on its boundary, there is either a boundary edge of R or a mountain edge of the lift (or both) that is incident to p_i and contained in H . See Figure 14a.*

In particular, if p_i is an interior vertex, then the mountain edges must surround p_i in a nonpointed manner.

For vertices in general position, this statement can be rephrased as: “Then, p_i is relative nonpointed in the graph consisting of boundary edges of R and mountain edges of the lift”. We need the more careful statement for cases where collinear edges arise naturally (see Lemma 4.10 and Figure 15(b)).

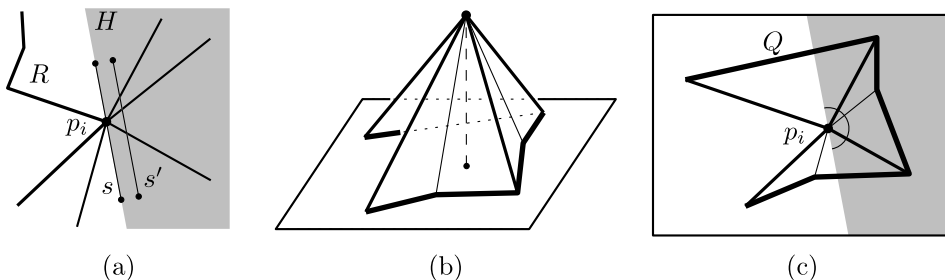


FIGURE 14. (a) At least one of the three edges pointing from the maximum point p_i into H must be a mountain edge. (b) Cutting the surface below the maximum. Mountain edges are drawn thicker than valley edges. (c) The projected intersection Q . Mountain edges become convex vertices and valley edges become reflex vertices of Q .

PROOF. Let s be a line segment through p_i on the boundary of H . Consider a segment s' parallel to s that is slightly pushed into H . If H contains no mountain edges incident to p_i , the lifting f must be a convex function on s' . Pushing s' towards s , we conclude that f is convex on s , and hence p_i cannot be a strict local maximum.

Another, more visual proof is illustrated in Figure 14b–c. Let us cut the lifted surface with a horizontal plane slightly below the maximum point p_i . The intersection projects to a polygonal chain Q that has a vertex on every edge incident to p_i . It follows that Q must contain a convex vertex in every 180° angular range that lies within R . Since convex vertices of Q result from mountain edges, the lemma is proved. \square

4.4. Flipping to Local Convexity. Let us now come back to the problem discussed at the start of this section: we have a pointgon (R, P) with given height values h_i at the points $p_i \in P$, and we look for the highest locally convex function f above R that does not exceed these heights. We have seen that such a function is uniquely defined once we fix a pseudo-triangulation T of (R, P) . (The given height values at the relative pointed vertices are simply ignored.) T may not use all interior points of R , i. e., it can be a pseudo-triangulation of (R, P') with $P' \subseteq P$. The resulting function will, in general, not be locally convex, and it may not respect the given heights at the relative pointed vertices and at the points of $P - P'$. But, if f happens to have these properties, it is the solution of our problem.

Lemma 4.9. *Let T be a pseudo-triangulation (R, P') with $P' \subseteq P$ and let $f: R \rightarrow \mathbb{R}$ be the function that is uniquely defined by the heights of the relative nonpointed vertices of T according to Theorem 4.4. If*

$$(3) \quad f(p_i) \leq h_i, \text{ for all } p_i \in P.$$

and no interior edge of T is lifted to a mountain edge, then f is the highest locally convex function that satisfies (3).

PROOF. (Sketch) In any locally convex lifting, the heights $z_i = f(p_i)$ must satisfy (2) as an inequality

$$(4) \quad z_l \leq \lambda_i z_i + \lambda_j z_j + \lambda_k z_k$$

if p_l is a vertex of a pseudo-triangle of T with corners p_i, p_j, p_k . One can show, by a monotonicity argument similar to the proof of Theorem 4.4, that the highest values z_i that fulfill (4) for all pseudo-triangles of T and (3) for all relative nonpointed vertices of T must fulfill these inequalities as equations, and hence they coincide with the function f defined by Theorem 4.4. \square

The following algorithm finds the appropriate pseudo-triangulation by a sequence of flipping operations. We start with an arbitrary triangulation of (R, P) . Then all vertices are relative nonpointed, and (3) is satisfied with equality. We will maintain (3) throughout. As long as some interior edge e of T is lifted to a mountain edge, we try to improve the situation by flipping the edge e , leading to another pseudo-triangulation T' .

- (1) If the flip is a diagonal-edge flip, T and T' have the same set of relative nonpointed vertices.
- (2) If the flip is an edge-removal, T' has one relative nonpointed vertex less than T . Theorem 4.4 still applies, and the height of the new relative pointed vertex is derived from the (given) heights of the relative nonpointed vertices.

We remark that in contrast to flipping in triangulations, an edge flip has a non-local effect on the lifting f . The flipping operation affects not only the faces incident to e , but it modifies the system of equations (2) and may change the

heights of other relative pointed vertices. However, we can predict the direction of this change: We say that the flip is *downward* if the edge e was a mountain edge. That is, if f is locally concave in the neighborhood of e .

Lemma 4.10. *After a downward flip from T to T' , the new lifting f' is everywhere weakly below the original lifting f . That is, for every point $x \in R$, $f'(x) \leq f(x)$.*

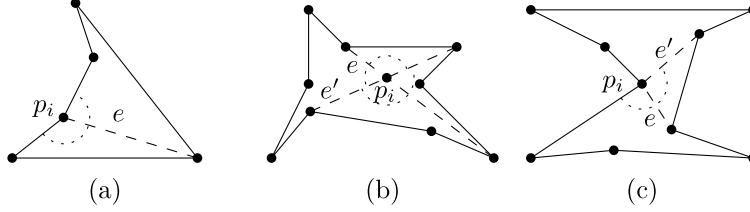


FIGURE 15. (a) an edge removal flip; (b) (c) two types of diagonal flip

PROOF. Let T'' be the pseudo-triangulation obtained by superimposing the edges of T and T' , see Figure 15. There are several possible cases, but in all of them T'' has exactly one more relative pointed vertex p_i than T' : in an edge removal flip, $T'' = T$ and p_i is the end-point of e that changes from non-pointed to pointed. In a diagonal flip, p_i is the intersection of the deleted and inserted edge (Figure 15a). The intersection is either an interior point of both (then a new vertex in T'' , Figure 15b) or an end-point of both (Figure 15c), then a pointed vertex of T and T' that becomes non-pointed in T'').

By the definition of f' , p_i is the only relative nonpointed vertex of T'' that has different height in f and f' .

Consider the family of liftings obtained for varying heights h_i of p_i , keeping the height of every other relative nonpointed vertex of T'' fixed. If we set $h_i = f(p_i)$ we get the original lifting: the edge e' (if it exists) is lifted to a flat edge. For $h_i = f'(p_i)$, we get the new lifting in which e is flat. By the monotonicity stated in Theorem 4.4, we only need to prove that $f(p_i) > f'(p_i)$.

Start with h_i very high and gradually move h_i downward. We know from Lemma 4.7 that p_i is initially the unique maximum point. If we look at the three cases of Figure 15 we see that e lies always in some 180° region around p_i with no other edges incident to p_i . Hence, by Lemma 4.8, e (or the two segments of e) must be a mountain edge. The height of every point in the lifting depends linearly on h_i , hence e is a mountain edge for all $h_i > f'(p_i)$, it is a flat edge at $h_i = f'(p_i)$, and a valley edge below $f'(p_i)$. Since e was assumed to be a mountain edge at $h_i = f(p_i)$, we have $f(p_i) > f'(p_i)$. \square

This lemma implies that by performing downward flips we will eventually arrive at a locally convex function.

Theorem 4.11. *For any given set of heights h_i of a pointgon (R, P) , the process of flipping downwards leads, in a finite number of steps, to a pseudo-triangulation T_0 and a lifting f which is the highest locally convex function on R below the values h_i .*

PROOF. In the process of flipping downwards no pseudo-triangulation can be visited twice, by the monotonicity proved in Lemma 4.10. Eventually, we must arrive at a pseudo-triangulation T_0 whose associated lifting function f is locally convex. We started with a triangulation of (R, P) , where every vertex of P was lifted to the given height h_i . By construction, f can only decrease in each step, and thus it is never above the given heights h_i . At the relative nonpointed vertices, we have $f(p_i) = h_i$. Hence, by Lemma 4.9, f is the desired lifting. \square

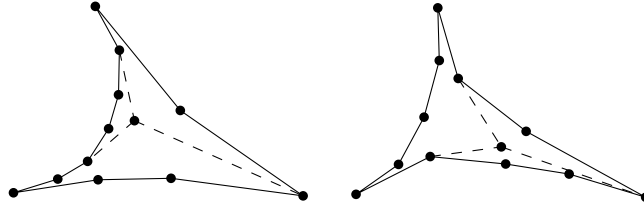


FIGURE 16. Two situations where an edge-removal flip for any of the three dashed edges will cause the two other edges to become flat. This is equivalent to removing the common vertex and merging the incident faces into one.

The lifting f in the above statement is unique, but the pseudo-triangulation T_0 may not be unique for the following reason: interior vertices may become flat and will remain so for the rest of the process. Then, the flat union of pseudo-triangles obtained in the final pseudo-triangulation may be different depending on the initial pseudo-triangulation, or even on the chosen path of flips. To avoid this ambiguity, we need a fourth type of flip that is performed as soon as a vertex gets degree two: the *vertex removal flip* removes this vertex and its two incident edges, merging two pseudo-triangles into one [5]. In particular, if we have a pointed interior vertex of degree 3, an edge-removal flip for any of the incident edges will cause this situation to occur, and we might as well remove the degree-3 vertex right away. Figure 16 shows this situation. The converse of a vertex-removal flip inserts a degree-3 vertex into the interior of a pseudo-triangular face, connecting it by geodesic paths to the three corners of that face. Observe that the result of a vertex removal is a pseudo-triangulation of a *different pointgon*, with the same polygon R but one point less in its interior.

It is not known whether the process of Theorem 4.11 terminates after a polynomial number of iterations. In the proof, we have shown that no pseudo-triangulation can show up twice in the process, but particular edges can in principle appear and disappear several times. (An example is given in [5].) Only for a convex domain R , where we have just triangulations and no pseudo-triangles, it can be guaranteed that no edge disappears and reappears, implying a quadratic upper bound on the number of downward flips needed to get the lower envelope.

More significant for us is the fact that the lower locally convex hull over a domain R gives rise to a pseudo-triangulation:

Theorem 4.12 (Aichholzer et al. [2]). *If the points p_i of a pointgon (R, P) and their given heights h_i are generic, the regions of linearity of the lower locally convex hull are pseudotriangles, and they form a pseudo-triangulation T of (R, P') for a subset $P' \subseteq P$ of vertices.*

Moreover, every interior vertex of T is non-pointed. □

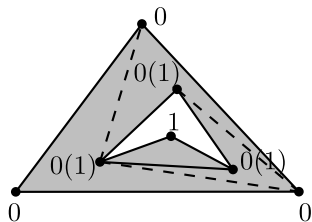


FIGURE 17. In a region R (shaded) that is not simply connected, the folding edges of the highest locally convex function may not create a pseudo-triangulation. The numbers indicate the heights z_i in the lower locally convex hull. The numbers in parentheses indicate the given heights h_i , whenever they are different from the final heights z_i . There is a face at $z = 0$ which is not a pseudo-triangle. (It is not even a simple polygon.) Perturbing the heights or the vertices will not change this situation.

When the region R is not a simple polygon, we leave the realm of pseudo-triangulations, see Figure 17. The characterization of the graphs that can arise (generically) as the edge sets of locally convex functions (or of general piecewise linear functions) over such general polygonal domains is still an open problem. Some results in this direction are given in [2, Section 8].

5. Self-Stresses, Reciprocal Diagrams, and the Maxwell-Cremona Correspondence

5.1. Maxwell liftings of pseudo-triangulations of point sets. Maxwell's Theorem (stated below) is a classical result relating three objects for a given geometric graph G : its 3D liftings, its planar reciprocal diagrams, and its equilibrium stresses. Let G be a connected geometric non-crossing graph.

Reciprocal diagrams: A geometric graph G' is called a *dual* of G if there is an incidence-preserving bijection from faces and edges of G to vertices and edges of G' , respectively: G' has a vertex for each face of G . For every edge of G that is shared between two faces of G , G' has an edge between the corresponding vertices. G' is called a *reciprocal diagram* of G if each edge of G is parallel to the corresponding edge of G' . A reciprocal diagram G' is not necessarily non-crossing. As a boundary case we also allow vertices of G' to coalesce. (A zero-length edge of G' is by definition considered to be always parallel to the corresponding edge of G .)

Maxwell liftings: A Maxwell lifting of G is a 3D lifting in the sense of Definition 4.1, where the outer face is lifted to the horizontal plane $z = 0$.

Equilibrium stresses: Let P and E be the sets of vertices and edges of G . An equilibrium stress (or self-stress) of G is an assignment of a scalar $\omega_e = \omega_{ij} = \omega_{ji}$ to every edge $e = ij$ of G such that every vertex “is in equilibrium”: We think of the edge ij as exerting a force $\omega_{ij}(p_j - p_i)$ on the vertex i (and an opposite force on j). The forces at every vertex i must add up to zero:

$$(5) \quad \sum_{j \mid \{i,j\} \in E} \omega_{ij}(p_j - p_i) = 0.$$

In Section 6, equilibrium stresses will be related to rigidity.

Theorem 5.1 (Maxwell [30, 31]). *For every connected geometric non-crossing graph G there is a one-to-one correspondence (bijection) between*

- (1) *reciprocal diagrams of G in which the dual vertex of the outer face is at the origin;*
- (2) *equilibrium stresses on G ; and*
- (3) *Maxwell liftings of G .*

This bijection is a linear isomorphism between the corresponding vector spaces. \square

The equivalence between reciprocal diagrams and equilibrium stresses is very easy to formulate: From a given reciprocal diagram G' we associate to each edge e the (signed) quotient between the length of the edge e' reciprocal to e and the edge e itself. The sign must be chosen following the following rule (or the opposite one): consider the edge e oriented from i to j , and give the same orientation to the parallel edge e' . If the cell dual to i is to the right of e' we choose a positive sign for the scalar. Otherwise, we choose it negative. Conversely, if an equilibrium stress is given in G , the graph G' can be drawn as follows. If the edges around a vertex i are e_1, \dots, e_k , in cyclic order, the boundary of the cell dual to i in G' consists of the cycle of edges $\omega_1 e_1, \dots, \omega_k e_k$. The equilibrium condition on i guarantees that this cycle of edges ends at the starting point. It is not difficult to show that the cells obtained in this way for the different vertices glue well, and give a non-crossing graph G' . See an example in Figure 18.

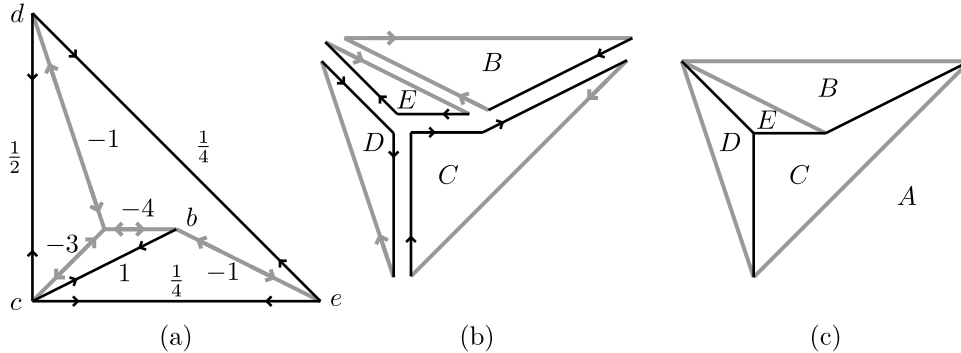


FIGURE 18. Assembling the reciprocal

The relation between equilibrium stresses and Maxwell liftings is a bit more difficult to show. The stress associated to a given edge e is related to the difference between the normal vectors to the liftings of the two cells incident to e . In particular, the sign of an edge in the stress indicates whether the edge is a mountain or valley edge in the lifting. Edges with stress 0 are lifted to flat edges.

Let us look back at the Surface Theorem (Theorem 4.4) in the context of Maxwell liftings, for the case when the boundary of the graph G (i.e., the contour of the outer face) is a convex polygon. Then the relative nonpointed vertices are just non-pointed vertices (which lie necessarily in the interior). Moreover, if G is a pseudo-triangulation then it is “a pseudo-triangulation of a point set”.

Corollary 5.2. *Let T be a pseudo-triangulation of a point set P . Then, for every choice of height on the non-pointed vertices of T there is a unique Maxwell lifting of T . Moreover, the height of every point depends linearly and monotonically on the heights of the non-pointed vertices, and the maximum of the lifting is achieved either on the boundary or at a non-pointed vertex, for every choice.*

Specially interesting is the case of pseudo-triangulations with a unique non-pointed vertex. We call them “almost-pointed”.

Corollary 5.3. (a) *An almost-pointed pseudo-triangulation of a point set has a unique reciprocal diagram, and a unique Maxwell lifting, modulo scaling and translation.*

(b) *A pointed pseudo-triangulation of a point set has only the trivial Maxwell lifting, and it has only the “degenerate” reciprocal diagram, where all vertices coalesce.* \square

5.2. Non-crossing graphs with non-crossing reciprocals. If one draws an example of an almost-pointed pseudo-triangulation and computes its unique reciprocal, the outcome will be another almost-pointed pseudo-triangulation. To understand this phenomenon, Orden et al. [34] studied the precise conditions that are sufficient and necessary for a non-crossing graph with a given stress to produce a non-crossing reciprocal. Their main result is the following characterization of when this happens via the type of vertices (pointed or not) and the sign changes in the equilibrium stress. In the statement, a *sign change* at a face or a vertex is a pair of consecutive edges (in the cyclic order along the boundary of the face or around the vertex) whose stress has opposite sign.

Theorem 5.4 ([34]). Vertex conditions for a planar reciprocal. *Let G be a non-crossing geometric graph with given self-stress ω . Then, in order for the reciprocal diagram G' to be also non-crossing, the following vertex conditions on its vertex cycles are necessary and sufficient:*

- (1) *there is a non-pointed vertex with no sign changes.*
- (2) *all other vertices are in one of the following three cases:*
 - (a) *pointed vertices with two sign changes, none of them at the big angle.*
 - (b) *pointed vertices with four sign changes, one of them at the big angle.*
 - (c) *non-pointed vertices with four sign changes.*
- (3) *the face cycles reciprocal to the vertices of type 2.c are themselves non-crossing.*

Face conditions for a planar reciprocal. *The four types of vertices produce, respectively, the following types of faces in G' :*

- (1) *the (complement of) the exterior face, which is strictly convex with no sign changes.*
- (2) *the internal faces of G , which are either*
 - (a) *pseudo-triangles with two sign changes, both occurring at corners.*
 - (b) *pseudo-triangles with four sign changes, three occurring at corners.*
 - (c) *pseudo-quadrangles with four sign changes, all occurring at corners.*

In particular, for a non-crossing framework to have a non-crossing reciprocal it is necessary that its faces fall into these four categories.

PROOF. (Sketch.) The proof of the two sets of conditions is intertwined, and consists of the following steps. First, necessity of the face conditions is shown by

a local argument: for a given face, the reciprocal vertex can potentially produce a non-crossing reciprocal only if the sum of angles reciprocal to those of the face equals 2π , and this can be seen to be equivalent to satisfying one of the face conditions. From this, necessity of the vertex conditions is also derived, since they are reciprocal to the face conditions. Also, a counting argument shows that the vertex conditions (1) and (2) imply the corresponding face conditions (for the original graph, not only for the reciprocal). In vertices of types 1, 2.a and 2.b, the reciprocal face is automatically non-crossing, because it is either a convex polygon or a pseudo-triangle. However, the vertex condition 2.c can in principle produce a *self-intersecting pseudo-quadrilateral*, see Figure 19b, but this is ruled out by condition (3). Finally, a topological argument shows that if all face cycles reciprocal to the vertices of G are non-crossing, then the reciprocal diagram is globally non-crossing, proving sufficiency of the vertex conditions. \square

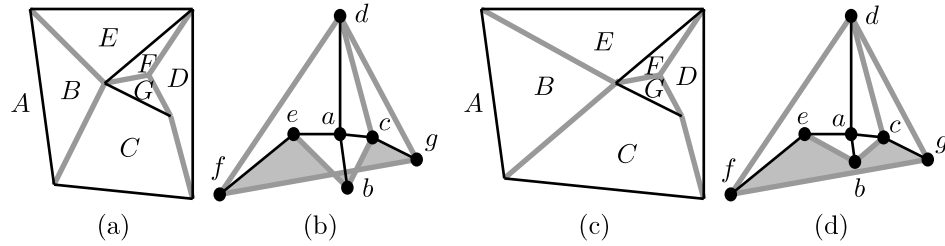


FIGURE 19. Sign conditions are not enough to guarantee a planar reciprocal. The two graphs in (a) and (c) have both the self-stress with signs represented in the figure by grey and black edges. The reader can visualize the Maxwell lifting: the outer face is at height 0, and if a height is chosen for the common vertex of faces B , C and E , then there is a unique Maxwell lifting compatible with that choice. The signs in the stress indicated whether the edges are mountain or valley edges in the lifting. The reciprocal diagrams are shown in (b) and (d). One is non-crossing but the other is not.

Let us come back to pseudo-triangulations.

Corollary 5.5 ([34]). *Let G be a pseudo-triangulation with a unique non-pointed vertex, and let ω be its unique self-stress. If ω is non-zero on every edge, the reciprocal diagram G' is again an almost-pointed pseudo-triangulation. The reciprocals of the outer face and non-pointed vertex of G are the non-pointed vertex and outer face of G' .*

PROOF. (Sketch.) The equilibrium condition at a pointed vertex implies that around the vertex there must be at least two sign changes, and at least four if one of them is at the reflex angle. A careful accounting of these sign changes proves that these bounds must be exact, and the possible patterns of sign changes (and sign non-changes) around each vertex and around each face are exactly equivalent to conditions 1 and 2 for vertices and for faces in Theorem 5.4. \square

If the self-stress ω has zeroes, the corresponding zero edge becomes flat in the corresponding Maxwell lifting (its two incident faces are coplanar) and it degenerates to length zero in the reciprocal diagram. It turns out that the previous corollary generalizes to this case:

Proposition 5.6 ([34]). *Let G be a pseudo-triangulation with a unique non-pointed vertex, and let ω be its unique self-stress. Then, the reciprocal diagram G' of G is a pseudo-triangulation.*

More precisely, let G^ be the subgraph consisting of the edges of G with non-zero ω . Then, G^* is a pseudo-quadrangulation (subdivision of a convex polygon into pseudo-triangles and pseudo-quadrangles). If G^* has n vertices and k pseudo-quadrangles, G' will be a pseudo-triangulation with $n-1$ pseudo-triangles and $k+1$ non-pointed vertices.* \square

There is a sort of converse of this statement:

Proposition 5.7 ([34]). *If a pseudo-triangulation G with a non-zero self-stress ω produces a non-crossing reciprocal G' , then G' can be extended to an almost-pointed pseudo-triangulation whose unique self-stress is non-zero exactly at the edges of G' .* \square

We finally mention several interesting properties of the unique, up to scaling in the vertical direction, Maxwell lifting of a non-crossing framework with a non-crossing reciprocal. We can assume, by changing the sign if necessary, that the lifting contains points above the zero plane. These properties are proved in [34]:

- The local and global minima are precisely the points in outer face, including the boundary.
- The unique local maximum is the distinguished non-pointed vertex whose reciprocal is the outer face of G' . Moreover, all edges around this vertex are mountain edges.
- The maximum is the only point having a supporting plane which leaves the surface f (locally) on one side of it.
- For every height h between the minimum and the maximum, the level curve of f at height h is a simple cycle. In particular, f has no saddle points.
- However, in every vertex v other than the maximum, the surface is negatively curved in the following sense: there is a plane passing through v that cuts f into 4 pieces in a neighborhood of v . (In other words, v is a *tilted saddle point*.)

6. Rigidity of Pseudo-Triangulations

In this section, we look at geometric graphs as bar-and-joint *frameworks*. The edges are treated as *rigid bars* (they maintain their lengths) and are allowed to rotate about their incident vertices (called *joints*). Intuitively, such frameworks are *flexible* or *rigid*, depending on whether their shape changes or not during motions. (Precise definitions are given below.) The main result of this section is that *pointed pseudo-triangulations* are always rigid, and when one of their convex hull edges is removed, they become flexible *mechanisms* with one degree of freedom, which move expansively (increasing the distance between any pair of joints).

The section is largely self-contained, but for additional background terminology and fundamental results in rigidity theory, we refer the reader to [23, 43, 57, 56].

6.1. Pointed pseudo-triangulations are generic minimally rigid frameworks. We have seen in Section 2.3 that the underlying graphs of pointed pseudo-triangulations are *Laman graphs*: their number of edges is $2n - 3$, and each induced subgraph on n' vertices spans no more than $2n' - 3$ edges. A classical result in rigidity theory (briefly surveyed below) implies that *generically* (i.e., in almost all embeddings), frameworks built from Laman graphs are *minimally rigid*: they are rigid but the removal of *any* edge produces a flexible object.

We start by reviewing the necessary concepts from rigidity theory.

Rigid and flexible frameworks. Given a geometric graph G embedded on the point set $P = \{p_1, \dots, p_n\}$, determine its edge lengths ℓ_{ij} , ($ij \in E$) and keep them fixed. Call the pair (G, P) a *framework*. The collection of all realizations (G, P') producing the same edge lengths is called the *configuration space* of the framework (G, P) . It is an algebraic subset of \mathbb{R}^{2n} , since it can be described as the set of all real solutions of the quadratic system

$$(x_i - x_j)^2 + (y_i - y_j)^2 = \ell_{ij}^2, \quad ij \in E,$$

where the pair of unknowns (x_i, y_i) denotes the position of the i th vertex of P' . Since an isometry applied to any solution leads to another solution, it is customary to fix (“pin down”) an arbitrary edge of G . Algebraically, if we assume it to be the edge 12, this amounts to add the equations $(x_1, y_1) = p_1$ and $(x_2, y_2) = p_2$ to the quadratic system. This reduces the dimension of the configuration space by three (not four, since it makes the equation between vertices 1 and 2 redundant).

A framework (G, P) is *rigid* if it is an isolated point in its configuration space. Otherwise, the framework is *flexible*.

Continuous Flexes. A *flex* or *reconfiguration* of a framework (G, P) is a continuous curve in its configuration space. That is, it is a function $P(t) = (p_1(t), \dots, p_n(t))$ defined over some interval of time, with

$$(6) \quad \|p_i(t) - p_j(t)\| = \ell_{ij}$$

for all edges $ij \in E$ and with $P = P(0)$. Again, to avoid trivial flexes we assume that a certain edge is fixed: $p_1(t) = p_1(0)$ and $p_2(t) = p_2(0)$, for all t .

Generic rigidity. Different frameworks realizing the same abstract graph can have different rigidity properties, as illustrated in Figure 20. The abstract graph is called *rigid* if *almost all* its embeddings are rigid. Technically, “almost all” means that rigid embeddings are a dense subset of the space \mathbb{R}^{2n} of all embeddings. A graph is *minimally rigid* if it is rigid but the removal of *any* edge invalidates this property.

The fundamental theorem of Rigidity Theory in the plane can now be stated:

Theorem 6.1 (Laman [28]). *A graph is minimally rigid iff it is a Laman graph.*

A framework is *generically rigid* if its underlying graph is rigid. Corollary 2.7 in Section 2.3 leads to the first fundamental rigidity property of pseudo-triangulations:

Corollary 6.2. *Every pointed pseudo-triangulation of a point set is generically minimally rigid.*

This already implies that the removal of an edge from a pointed pseudo-triangulation produces a framework that, generically, is flexible.

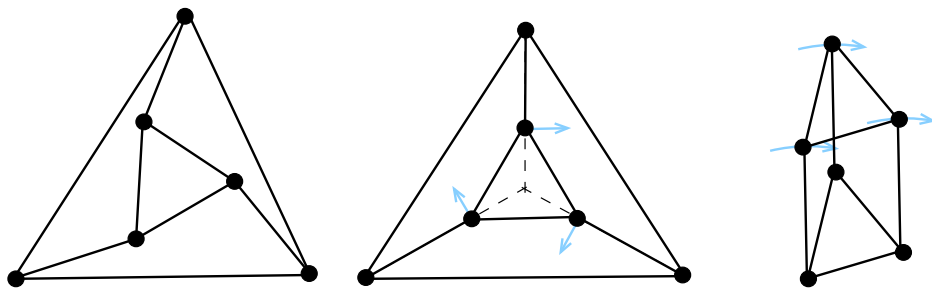


FIGURE 20. Different embeddings of the same graph (in this example, a rigid graph) can have different rigidity properties: infinitesimally rigid and therefore also rigid (left), rigid but infinitesimally flexible (center), or flexible (right).

6.2. Pointed pseudo-triangulations are infinitesimally rigid. Being *generically* minimally rigid is already a distinguishing graph-theoretic property of pointed pseudo-triangulations. We show next that they are not just rigid in *almost all* embeddings, but that they are rigid in *all* embeddings as pseudo-triangulations. To prove this, we introduce the important concept of *infinitesimal rigidity*. Infinitesimal rigidity implies rigidity, and, being based on linear algebra, it is much easier to prove.

Infinitesimal rigidity. An *infinitesimal motion* or *infinitesimal flex* of a framework (G, P) is a family of velocity vectors $v = (v_1, \dots, v_n)$, $v_i \in \mathbb{R}^2$ which preserve the lengths of all edges $ij \in E$, to first order:

$$(7) \quad \langle p_i - p_j, v_i - v_j \rangle = 0, \forall ij \in E$$

Formally, these equations are obtained from (6) for the moving points $p_i(t)$ by taking the derivative with respect to t , with $v_i(t) = \dot{p}_i(t)$, up to a constant factor. As with continuous flexes, to neglect infinitesimal translations (in which all v_i are equal) and rotations (in which every v_i is orthogonal and proportional in length to $\overrightarrow{Op_i}$ for some fixed point O) we pin down an edge. This now means that we set $v_1 = v_2 = 0$, where we assume that $12 \in E$. A framework (G, P) is *infinitesimally rigid* if it has no (non-trivial) infinitesimal motion.

If $P(t)$ is a continuous and differentiable flex of a framework (G, P) (with $P = P(0)$), then the first derivative of $P(t)$ at $t = 0$ is an infinitesimal flex of the framework. In particular, infinitesimally rigid frameworks are rigid: since the configuration space of a framework is algebraic, existence of a continuous motion implies existence of a differentiable (even analytic) motion and hence of an infinitesimal motion. As an example that the converse is not true we have the second embedding in Figure 20. The framework is rigid but, still, the interior triangle can be “infinitesimally rotated” with respect to the exterior one.

Since infinitesimal rigidity is a linearized version of rigidity, it can very nicely be understood in matrix form. The $2n \times m$ coefficient matrix M of the equations (7) is called the *rigidity matrix* associated to the framework (G, P) . The set of infinitesimal motions is the kernel of M , and thus a linear subspace in $(\mathbb{R}^2)^n \simeq \mathbb{R}^{2n}$. This set contains the three-dimensional linear subspace of *trivial motions* (infinitesimal rotations and translations) and a framework is infinitesimally rigid if and only if the kernel of its rigidity matrix has dimension three. We say that

(G, P) has d (*internal*) *infinitesimal degrees of freedom* if the space of infinitesimal motions has dimension $d + 3$.

Pseudo-triangulations are infinitesimally rigid. Infinitesimal rigidity of a framework is related to the equilibrium stresses introduced in Section 5.1 by the following classical result:

Theorem 6.3. *Let (G, P) be a framework in the plane with n vertices, m edges, d infinitesimal degrees of freedom and a space of self-stresses of dimension s . Then,*

$$m = 2n - 3 + (s - d).$$

PROOF. Comparing the system (7) with the system (5) of Section 5.1 one sees that equilibrium stresses form the kernel of the transpose of the $2n \times m$ rigidity matrix M . Let the rank of M be r . Since $d + 3$ and s are the kernel dimensions of M and its transpose, we have

$$r = m - s = 2n - (d + 3). \quad \square$$

The following consequence of this theorem was first proved by Streinu [53] for the pointed case and by Orden and Santos [35] in general. Our proof uses the Surface Theorem (Theorem 4.4) of Aichholzer et al.

Theorem 6.4. *Every pseudo-triangulation of a point set is infinitesimally rigid, hence rigid. Pointed pseudo-triangulations are minimally infinitesimally rigid.*

PROOF. By Corollary 4.5, together with Maxwell's Theorem 5.1, the dimension s of the space of equilibrium stresses of a pseudo-triangulation equals its number n_χ of non-pointed vertices. Since a pseudo-triangulation on n vertices has $2n - 3 + n_\chi$ edges, the previous theorem implies that it has no non-trivial infinitesimal motions. \square

Observe that if a graph is infinitesimally rigid then its rigidity map has full rank for this embedding and, hence, for almost all embeddings of the same abstract graph, the rank can drop only on certain algebraic hypersurfaces in the configuration space. In particular, the pointed case of Theorem 6.4 implies Corollary 6.2. However, for non-pointed pseudo-triangulations we do not have a proof of their generic rigidity (that is, of the fact that they contain a Laman subgraph) other than via their infinitesimal rigidity. Not every pseudo-triangulation contains a pointed pseudo-triangulation.

6.3. Pointed Pseudo-Triangulation Mechanisms. If a framework is minimally infinitesimally rigid, the removal of any edge creates a flexible object with one infinitesimal degree of freedom. In this section we outline an even stronger property (from [53]), for the case of a pointed pseudo-triangulation with a convex hull edge removed: the resulting framework is a mechanism (with one degree of freedom) which *expands* all distances between its vertices when the endpoints of the removed convex hull edge are moved away from each other. We call these frameworks *pointed pseudo-triangulation mechanisms*.

Expansion and contraction. For a point set P and infinitesimal velocities v , we define the *expansion* ε_{ij} as follows:

$$(8) \quad \varepsilon_{ij} := \langle p_i - p_j, v_i - v_j \rangle$$

Formally, this expression is obtained as the derivative of $\frac{1}{2}\|p_i(t) - p_j(t)\|$ with respect to t . We say that the pair ij of points *expands* if $\varepsilon_{ij} \geq 0$ and *contracts* if $\varepsilon_{ij} \leq 0$. An infinitesimal motion is *expansive* if all pairs of vertices expand.

Expansive mechanisms. A mechanism is a framework (G, P) with a one-dimensional space of infinitesimal motions. Essentially, up to reversal, there is only one direction in which the mechanism can move. It is (infinitesimally) *expansive* if, in this motion (or its reverse), all pairs of vertices expand.

The following lemma results from the fact that the rigidity matrix is the transpose of the matrix of the system (5) defining self-stresses. The space of expansions ε_{ij} is the image of this matrix, and is thus orthogonal to the kernel of the transpose.

Lemma 6.5. *Let H be a Laman framework with an extra edge, and let ij and kl be two edges of H . Let $H' = H - \{ij, kl\}$. Let v be an infinitesimal motion of H' , and let ω be a self-stress of H . Then,*

$$\omega_{ij}\varepsilon_{ij} + \omega_{kl}\varepsilon_{kl} = 0 \quad \square$$

We can now prove the main result of this section:

Theorem 6.6 (Streinu [53]). *A bar-and-joint framework whose underlying graph is obtained by removing a convex hull edge from a pointed pseudo-triangulation is an expansive mechanism.*

PROOF. Let G be the underlying graph of the pointed pseudo-triangulation, ij be the removed convex hull edge (so that $G \setminus \{ij\}$ is a pointed pseudo-triangulation mechanism). Let v be an infinitesimal motion preserving the edge lengths of $G \setminus \{ij\}$ and increasing the length of the edge ij , $\varepsilon_{ij} > 0$. We want to prove that it also increases the distance of every other pair of vertices kl , i.e., $\varepsilon_{kl} \geq 0$.

Consider the graph $H = G \cup \{kl\}$. It has $2n - 2$ edges, and therefore, by a dimension argument, it supports a non-trivial self-stress ω . Since G itself supports no self-stress, we must have $\omega_{kl} \neq 0$. Without loss of generality, we assume $\omega_{kl} > 0$. Now, if we have $\varepsilon_{kl} < 0$, then Lemma 6.5 would imply $\omega_{ij} > 0$. Hence, it is sufficient to show that $\omega_{ij} > 0$ and $\omega_{kl} > 0$ leads to a contradiction. We will interpret the self-stress in terms of the induced Maxwell lifting to derive this contradiction.

Consider the framework $G \cup \{kl\}$ obtained from G by adding the extra edge $e = kl$. Since it is no longer a pointed pseudo-triangulation, either one endpoint or both endpoints of this new edge kl are non-pointed, or else the edge kl crosses some other edges of the pseudo-triangulation. If new crossings have been introduced, we will apply Bow's construction [32] to eliminate them: simply replace each crossing by a new vertex, and split the two crossing edges in two. We obtain a new planar framework G' , which will have n' vertices and $2n' - 2$ edges. In either case, the new framework is non-pointed only at one or both of the endpoints of e or at the crossings of e with other edges (or both). Denote by P_X the non-empty set of non-pointed vertices: the endpoints of e , if non-pointed, and the crossings of e with other edges, if there are such crossings.

The signs of the self-stresses are preserved by Bow's construction. Since we assumed a strictly positive self-stress on ij and $e = kl$, this means that both ij and e are valley edges in a Maxwell lifting of G' (and this extends to the split edges in case Bow's construction has been applied). The only edges which could be mountain edges are the edges of G .

Since the convex hull edge ij is a valley edge, the Maxwell lifting contains points above the outer face $z = 0$, so the maximum height be attained on some set M consisting of vertices, edges, and bounded faces of G' .

Let us look a convex hull vertex p of M . It follows from Lemma 4.2 that p must be a non-pointed vertex from P_X . Since all vertices of P_X lie on e , we know that M is a union of vertices and edges that lie above e . The edges lying above e are either e or splittings of e and have negative stress, therefore lift to valleys. Valleys cannot be maxima, obviously. Thus the maximum height is attained at a set M of isolated interior vertices.

To complete the proof, let us focus on one such vertex p_i of maximum height. By Lemma 4.8, the mountain edges, which must be edges of G , surround p_i in a non-pointed manner, contradicting the assumption that G is pointed. \square

In [53], additional rigidity theory apparatus is used to prove that this infinitesimal motion leads to an actual motion: a one-dimensional trajectory in configuration space, for a portion of which all vertices move away from each other. In Section 9.5, this property is used for an algorithmic solution to the Carpenter's Rule Problem.

Theorem 6.7 (Motion of pointed pseudo-triangulation mechanisms [53]). *A pointed pseudo-triangulation mechanism moves expansively on a unique trajectory, from the moment when a corner angle is zero to the moment when two extreme edges of a vertex (or, as a special case, when one of these is the missing convex hull edge) align.* \square

6.4. Parallel Redrawings of Pointed Pseudo-Triangulation Mechanisms. Two-dimensional rigidity theory has an alternative, equivalent model, called the theory of *parallel redrawings*, in which edges of frameworks are required to maintain their slopes instead of their lengths [57, 56]. It turns out that pointed pseudo-triangulation mechanisms are also special from the point of view of the theory of parallel redrawings: they are essentially the only frameworks for which all parallel redrawings are non-crossing. *Essentially* means that some of their rigid components may be replaced by arbitrary, not necessarily pointed, rigid frameworks but on the same point set.

A *parallel redrawing* of a geometric graph is one where corresponding edges have the same slopes. Naturally, any rescaling is a parallel redrawing, but this is not interesting: we call it *trivial*. Pointed pseudo-triangulation mechanisms are *flexible* from the point of view of parallel redrawings, i.e. they have non-trivial parallel redrawings. The following result summarizes the properties of pointed pseudo-triangulation mechanisms, as parallel-redrawing mechanisms.

Theorem 6.8 (Streinu [54]). *A pointed pseudo-triangulation with a convex hull edge removed has a one-dimensional projective space of non-trivial parallel redrawings. All of them are pointed pseudo-triangulation mechanisms with the same planar graph facial structure.* \square

Figure 21 illustrates a sequence of pseudo-triangulation parallel redrawings.

7. All Generically Rigid Graphs are Pseudo-Triangulation Graphs

We have seen in Theorem 6.4 that pseudo-triangulations of a point set are infinitesimally rigid. In particular, their underlying (abstract) graphs are generically

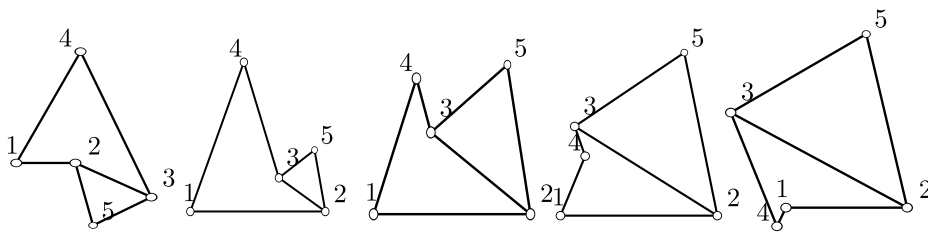


FIGURE 21. A few different parallel redrawings of a pointed pseudo-triangulation mechanism. The second and third snapshot have the same combinatorial structure (but are not trivial redrawings of each other). In all the others, some angle changes from convex to reflex or vice versa.

rigid in the plane. This section is devoted to the converse statement, proved in [24] or the Laman (i.e., minimally generically rigid) case and in [36] in the general case.

Theorem 7.1. *Every topological embedding of a generically rigid planar graph G can be stretched to become a pseudo-triangulation of a point set.*

This result is the analogue for pseudo-triangulations of Steinitz’s Theorem that every simple planar and 3-connected abstract graph is the graph of a 3-polytope, and in particular it can be drawn in the plane with convex faces and convex outer face. Here, instead of convex faces we draw graphs with faces that are “as non-convex as possible” (pseudo-triangles).

7.1. Combinatorial pseudo-triangulations. The proof of Theorem 7.1 relies on the concept of combinatorial pseudo-triangulation.

Definition 7.2. A *combinatorial pseudo-triangulation (CPT)* on a plane graph $G(P)$ is an assignment of labels *big* (or *reflex*) and *small* (or *convex*) to the angles (vertex-face incidences) of $G(P)$ such that:

- (i) Every face except the outer face gets exactly *three* vertices marked *small*. These will be called the *corners* of the face.
- (ii) The outer face gets only *big* labels (it has no corners).
- (iii) Each vertex is incident to at most one angle labelled *big*. The vertices incident to big angles are called *pointed*.

By analogy with pseudo-triangulations, we also define things like *non-pointed vertices*, *extreme edges* of a pointed vertex, corners and *pseudo-edges* of a pseudo-triangle, etc. CPT’s behave very much like true pseudo-triangulations. For example:

Lemma 7.3. *Every combinatorial pseudo-triangulation on n vertices has $2n - 3 + n_x$ edges, where n_x is the number of non-pointed vertices in it.*

PROOF. Use the counts of Theorem 2.1, which are purely combinatorial. \square

In particular, a CPT with exactly $2n - 3$ edges will have all vertices pointed. We call it a *pointed combinatorial pseudo-triangulation* (or pointed CPT).

Not all combinatorial pseudo-triangulations can be stretched:

- The one in the left of Figure 22 cannot be stretched since its graph is not generically rigid. (It has $2n - 3$ vertices but it is not a Laman graph.)
- The graph on the right is drawn as a true pseudo-triangulation, hence it is generically rigid. But its assignment of big and small angles is another combinatorial pseudo-triangulation. This CPT cannot be stretchable since the four boundary vertices and their two neighbors form a set of $n' = 6$ six pointed vertices whose induced subgraph has more than $3n' - 3 = 9$ edges. This is in disagreement with Corollary 2.8.

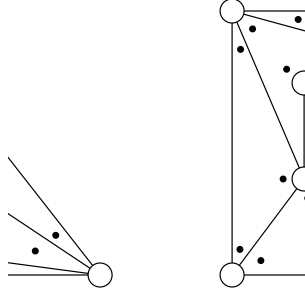


FIGURE 22. Two combinatorial pseudo-triangulations that are not stretchable. Dots represent angles labeled “small”.

The last example motivates the following definition:

Definition 7.4. A combinatorial pseudo-triangulation on a set V of n vertices is called a *generalized Laman CPT* if for every subset of $k \geq 2$ vertices in G , l of them non-pointed, the subgraph induced by these vertices has at most $2k - 3 + l$ edges.

This concept allows to decompose the proof of Theorem 7.1 into two parts:

Theorem 7.5. *Every rigid plane graph admits an angle labeling as a generalized Laman CPT.*

Theorem 7.6. *Every generalized Laman CPT is stretchable.*

7.2. Stretching combinatorial pseudo-triangulations. Here we sketch the proof of Theorem 7.6.

The 3-connected partially directed graph of a CPT. A *partially directed graph* $D = (V, E, \vec{E})$ is a graph (V, E) together with an assignment of directions to *some* of its edges. Edges are allowed to get two directions, one direction only, or remain undirected. Formally, \vec{E} is a subset of the set which contains two opposite directed arcs for each edge of E .

Lemma 7.7. *For every combinatorial pseudo-triangulation G , we can construct a partially directed graph D satisfying the following conditions:*

- (1) D is planar.
- (2) Every interior non-pointed vertex has as out-neighbors all its neighbors in G .
- (3) For an interior pointed vertex p of G , let Δ be the pseudo-triangle of G containing the big angle at p . The out-neighbors of p are the two neighbors of p in the boundary of Δ together with one vertex of Δ not lying in the same pseudo-edge as p .

PROOF. First we extend G by adding edges into every pseudo-triangle Δ that is not a triangle. For every interior big angle we add a directed edge through Δ towards some vertex not lying on the same pseudo-edge. This can be done in many different ways; one only needs to avoid crossings. The edges on the boundary of Δ are oriented as required by the statement. See Figure 23 for an illustration of the edges inserted and orientations given in a face Δ . Observe that a boundary edge incident to a corner of Δ may get a second orientation if the corner is non-pointed or if the corner is pointed and the edge is extremal. \square

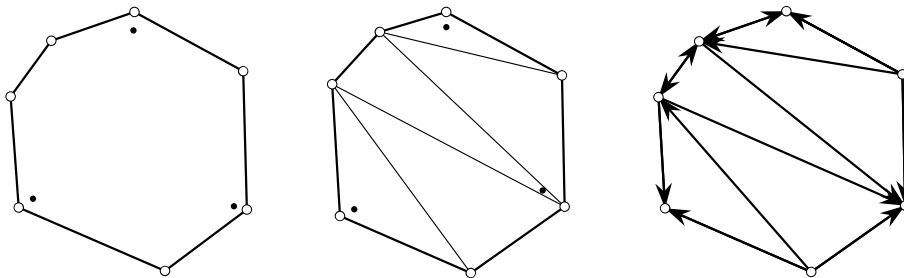


FIGURE 23. (a) A combinatorial pseudo-triangular face, with a small black dot indicating a small angle. (Big angles are not marked.) (b) One possible way for inserting the edges of the auxiliary directed graph. The dotted arrows indicate possible additional orientations for the boundary edges, depending on adjacent faces.

We say that a plane embedding of a partially directed graph (V, E, \vec{E}) is *3-connected to the boundary* if from every interior vertex there are at least three vertex-disjoint directed paths in \vec{E} ending in three different boundary vertices. The following statement follows from Theorem 6 in [36] and (part of) Theorem 7 in [24].

Theorem 7.8. *If a combinatorial pseudo-triangulation has the generalized Laman property, then the auxiliary graph constructed in Lemma 7.7 is 3-connected to the boundary.*

A directed version of Tutte's equilibrium method. To finish the proof of Theorem 7.6 we use a directed version of Tutte's Theorem on barycentric embeddings of graphs. An embedding $D(P)$ of a partially directed graph $D = (V, E, \vec{E})$ on a set of points $P = \{p_1, \dots, p_n\}$, together with an assignment $\omega: \vec{E} \rightarrow \mathbb{R}$ of weights to the directed edges is said to be in *equilibrium* at a vertex $i \in V$ if

$$(9) \quad \sum_{j: (i,j) \in \vec{E}} \omega_{ij}(p_i - p_j) = 0.$$

The following is Theorem 8 in [24]. Its proof is not very different from the proof of Tutte's Theorem given in [44, Theorem 12.2.2, pp. 123–132]. See the details in [18] or [24].

Theorem 7.9 (Directed Tutte Embedding). *Let $D = (\{1, \dots, n\}, E, \vec{E})$ be a partially directed plane graph, 3-connected to the boundary and whose boundary cycle*

has no repeated vertices. Assume $(k + 1, \dots, n)$ is the ordered sequence of vertices in this boundary cycle and let p_{k+1}, \dots, p_n be the ordered vertices of a convex $(n - k)$ -gon.

Let $\omega: \vec{E}' \rightarrow \mathbb{R}$ be an assignment of positive weights to the internal directed edges. Then:

- (i) There are unique positions $p_1, \dots, p_k \in \mathbb{R}^2$ for the interior vertices such that all of them are in equilibrium.
- (ii) These positions yield a straight-line plane embedding of D . All faces of D are (strictly) convex polygons. \square

We remark that the system (9) of equations for defining equilibrium is closely related to the system (2) for defining the heights z_i in a lifting of a pseudo-triangulation (Section 4.3). In fact, (9) decomposes into two independent systems, one for the x -coordinates of the points p_i , and one for the y -coordinates. Uniqueness of the heights in the Surface Theorem (Theorem 4.4) can be derived as a consequence of the unique solvability of (9).

PROOF OF THEOREM 7.6. From our combinatorial pseudo-triangulation we construct an auxiliary partially directed graph D in the conditions of Lemma 7.7, and choose arbitrary positive weights for its directed edges. By Theorem 7.8 this graph is 3-connected to the boundary, so that we can embed it in equilibrium and with convex faces, by the Directed Tutte Embedding Theorem. Since all weights are positive, the equilibrium condition implies that every interior vertex is in the relative interior of the convex hull of its out-neighbors.

The conditions on D then imply that the straight-line embedding of G so obtained has big and small angles distributed as desired: indeed, for a non-pointed vertex, all its out-neighbors are taken among the edges of G , hence the equilibrium implies that all incident angles are small. For a pointed vertex p_i , its three out-neighbors are its extreme neighbors in the CPT plus a vertex of the same pseudo-triangle that is not a neighbor of p_i in G , which implies that the angle of p_i in that pseudo-triangle is bigger than 180 degrees. \square

7.3. Generalized Laman CPT Labelings of Rigid Graphs. Here we sketch the proof of Theorem 7.5. That is, we show how to construct a generalized Laman CPT labeling of the angles of any topologically embedded generically rigid graph G . In the next section we show an alternative method that works if G is minimally generically rigid, that is to say, a Laman graph.

The general idea in the proof is to mimic combinatorially the Henneberg incremental construction of pseudo-triangulations described in Theorem 2.12. The case when G has a vertex p_0 whose removal still leaves a rigid graph is easy:

Lemma 7.10 ([36, Lemma 5]). *If $G \setminus p_0$ is rigid, then from any CPT labeling of $G \setminus p_0$ can be extended to a CPT labeling of G . If the former has the generalized Laman property, the latter does too.*

By “extended” we mean that angles of $G \setminus p_0$ that are not divided by the insertion of p_0 keep their labelings.

PROOF. Let Δ be the region of $G \setminus p_0$ where p_0 needs to be inserted. This region will either be a pseudo-triangle (of the CPT labeling of $G \setminus p_0$) or the exterior region of the embedding. There are the following cases. For each, Figure 24 shows the assignment of labels:

- (a) Δ is the unbounded region.
- (b) All neighbors of p_0 lie in a pseudo-edge of Δ .
- (c) p_0 has neighbors in only two pseudo-edges of Δ .
- (d) p_0 has neighbors in the three pseudo-edges of Δ .

The last three cases can degenerate to have one or more corners of Δ among the neighbors of p_0 . In this case the two angles at that corner are labeled small.

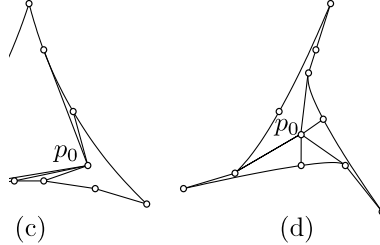


FIGURE 24. Several cases in the proof of Lemma 7.10. The labels are indicated implicitly by small and big angles in the drawing.

This labeling preserves the generalized Laman property: Firstly, no vertex changes from non-pointed to pointed. This implies that the generalized Laman property carries over from $G \setminus p_0$ to G for any subset of vertices not containing p_0 .

Secondly, all neighbors of the new vertex p_0 , except two if p_0 is labeled pointed and three if p_0 is labeled non-pointed, change their status from pointed to non-pointed. Thus, for a vertex set containing p_0 , p_0 itself allows us to count the two or three edges incident to neighbors that do not change status, while the change of status of every other neighbor allows to count the edge incident to it. \square

Assume now that G is a generically rigid plane graph on n vertices, and that the removal of any vertex breaks rigidity. G being rigid implies that it contains a spanning Laman subgraph L with $2n - 3$ edges. L must have vertices of degree at most three, but cannot have vertices of degree two (because the removal of those keeps L , hence G , rigid). Thus, L must have a vertex p_0 of degree three, whose removal leaves $L \setminus p_0$, and $G \setminus p_0$, non-rigid with one generic degree of freedom.

Let p_1, \dots, p_3 be the neighbors of p_0 in G , numbered cyclically in the plane embedding of G . In the 1-degree-of-freedom motion of (a generic straight-line embedding of) $G \setminus p_0$ not all p_i can move rigidly, since otherwise the insertion of p_0 would not make the graph rigid. Hence, there is at least one pair p_i, p_j of neighbors of p_0 in G such that the insertion of the edge $p_i p_j$ in $G \setminus p_0$ produces a rigid graph. We say that $p_i p_j$ *restores rigidity* in $G \setminus p_0$.

By inductive hypothesis we can assume that the rigid (and plane) graph $G \setminus p_0 \cup \{p_i p_j\}$ admits a generalized Laman CPT labeling, and our task is to extend this labeling to a generalized Laman CPT labeling of G , with a method similar to that of Lemma 7.10. Obtaining a CPT labeling is relatively easy, with a method similar to that of Lemma 7.10. The problem is that the generalized Laman property cannot be guaranteed unless p_i and p_j are carefully chosen.

Lemma 7.11 ([36, Lemma 6 and Corollary 3]). *In these conditions there is a pair of neighbors p_i, p_j such that the edge $p_i p_j$ restores rigidity in $G \setminus p_0$ and such that any generalized Laman labeling of $G \setminus p_0 \cup \{p_i p_j\}$ can be extended to one of G .*

7.4. CPT Labelings via Matchings. As we have said in the previous section, the tricky part in the proof of Theorem 7.5 is not the existence of a CPT labeling for every generically rigid plane graph, but the existence of one that has the generalized Laman property.

Now suppose that G is *minimally* generically rigid, so that we want to embed it as a *pointed* pseudo-triangulation, by Lemma 7.3. In this case the generalized Laman property restricts to the usual Laman property, which is a property of the graph, so we need not care about the embedding.

Streinu et al. [24] take advantage of this fact and give two proofs of the fact that every plane Laman graph can be given a CPT assignment. The first proof proceeds by induction in a Henneberg-like way, similar to the arguments that we have sketched for the general case in the previous section, except that the insertion of the new vertex p_0 is done directly in the geometric embedding. The other proof establishes that a certain auxiliary bipartite graph has a matching. We include it here for its simplicity and because it has the advantage of being fully algorithmic.

Lemma 7.12. *Pointed CPT labelings of a plane connected graph G are in bijection with perfect matchings in the following bipartite graph H constructed from G : one part is the set V of vertices of G , and the other part has $d - 3$ nodes for each bounded face of degree d , and as many nodes for the outer face as its degree. The edges join each node p in V to all nodes corresponding to faces incident to p in the embedding.*

PROOF. The edges in H correspond to the assignment of reflex angles in G . In a pointed CPT labeling of a plane graph G each vertex gets a reflex angle and each face, of degree say d , gets $d - 3$ reflex angles, except for the outer face that gets d of them. \square

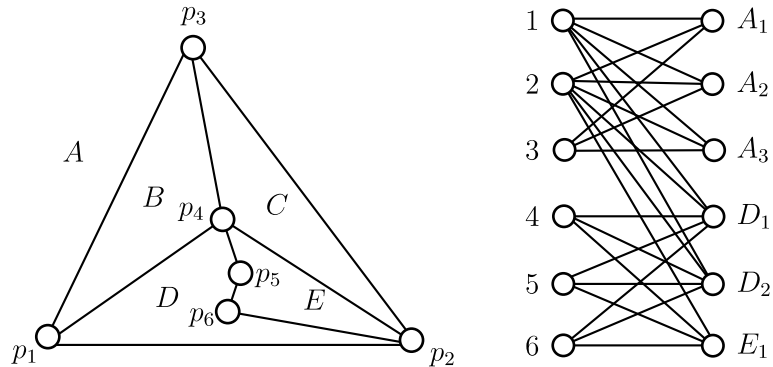


FIGURE 25. A plane graph with $2n - 3$ edges and its associated bipartite graph H .

We illustrate this result in Figure 25. The 6 vertices of the plane graph G on the left, and its 5 faces of degrees 3 (outer face A), 3 (faces B and C), 4 (face E) and 5 (face D) lead to the bipartition sets $V = \{1, 2, 3, 4, 5, 6\}$ and $W = \{A_1, A_2, A_3, D_1, D_2, E_1\}$, connected by edges as in the figure. That the two parts have equal sizes just reflects the fact that the number of edges in the graph equals $2n - 3$ (a necessary condition for existence of a CPT labeling, by Lemma 7.3). The

horizontal edges in the bipartite graph H form a perfect matching, which induces a pointed CPT labeling of G . Observe, however, that G is not a Laman graph; hence the CPT labeling is not a generalized Laman graph and, thus, it cannot be stretched.

Theorem 7.13 ([24]). *If G is a Laman graph, then H has a perfect matching. Hence G can be stretched to a pointed pseudo-triangulation with the same topological embedding.*

Let us mention that the proof of this result in [24] has a typographic error: the numbers of edges and vertices are swapped in formula (1).

PROOF. Let $W \subset V$ be a subset of $|W| = k$ vertices. Let F_W be the set of faces incident to the vertices in W , and R_W the union of those (closed) faces. Let $D = \sum_{f \in F_W} d_f$. Hall's condition for the existence of a perfect matching amounts to showing that $k \leq D - 3|F_W|$. (Actually, if one of the faces in F_W is the unbounded one, Hall's condition would be $k \leq D - 3|F_W| + 3$, but we will prove the stronger inequality anyway, assuming that F_W does not contain all faces.) The given vertices W lie in the interior of R_W .

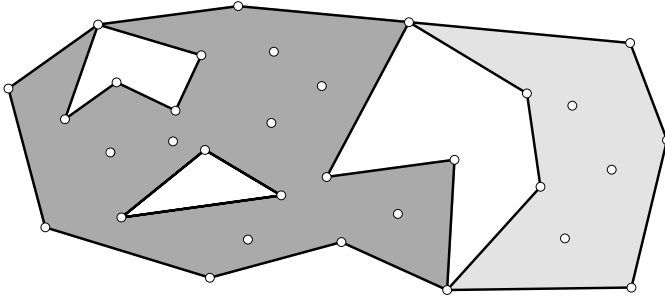


FIGURE 26. A region R_W which has two face-connected components, shaded differently. The one on the left has two holes, the white triangle and the white non-convex pentagon.

If R_W is not face-connected, we can prove the inequalities $k \leq D - 3|F_W|$ for each face-connected component separately and add them up. Thus, we assume from now on that R_W is face-connected. Then the region R_W is a polygon, perhaps with holes, see Figure 26. Let m_b and n_b be the number of edges and vertices of G that lie on the boundary of R_W , and let m_i and $n_i \geq k$ be those in the interior. Since $D = 2m_i + m_b$ it is sufficient to show

$$(10) \quad n_i \leq 2m_i + m_b - 3|F_W|.$$

Let h be the number of connected components in the complement of R_W . Euler's formula for the graph of all vertices and edges of G in R_W gives

$$(11) \quad (n_b + n_i) + (h + |F_W|) = (m_b + m_i) + 2.$$

We can also apply Euler's formula to the graph of boundary vertices and boundary edges. (These are the only edges that are shown in Figure 26.)

$$(12) \quad m_b + 2 \leq n_b + (h + 1)$$

(This is only an inequality since this graph may be disconnected.) The Laman property of G says that

$$(13) \quad m_b + m_i \leq 2(n_b + n_i) - 3.$$

We multiply (11) by 3, add (12) and (13), and after cancellation we obtain

$$n_i \leq 2m_i + m_b - 3|F_W| - 2h + 2.$$

Since $h \geq 1$ (using the fact that R_W does not contain all faces), (10) follows. \square

7.5. Pointedness and corners in plane graphs. We finish this chapter deriving from Theorem 7.1 a quite general statement about the possible number of pointed vertices in straight-line embeddings of planar graphs.

Let G be a connected planar (abstract) graph with n vertices and m edges. Let r be its generic rigidity rank. By this we mean the rank of the rigidity map in any generic (but not necessarily non-crossing) embedding of G . Knowing r is equivalent to knowing either the dimension s of the space of self-stresses or the number d of degrees of freedom, in generic embeddings of G . Indeed, by Theorem 6.3:

$$(14) \quad r + s = m = 2n - 3 + s - d.$$

Now let $G(P)$ be a straight-line embedding of G on a point set P in general position. By Theorem 2.9 we have the equation

$$(15) \quad m = 2n - 3 + n_\chi - \bar{k},$$

where n_χ is the number of non-pointed vertices and \bar{k} is the *excess of corners*, defined as the total number of convex angles in the embedding minus three times the number of bounded regions. That is, \bar{k} measures how far is G from being a pseudo-triangulation. By comparing the right-hand sides of (14) and (15), we get a relation between the rigidity-theoretic parameters s and d of the graph G and the parameters \bar{k} and n_χ in its plane embeddings.

Theorem 7.14. *Let G be a connected planar graph with (generically) an s -dimensional space of stresses and d infinitesimal degrees of freedom.*

(i) *In every non-crossing straight-line embedding $G(P)$ of G , one has*

$$n_\chi - \bar{k} = s - d, \quad \text{with } n_\chi \geq s \quad \text{and hence } \bar{k} \geq d.$$

(ii) *G has embeddings in which these bounds are attained: $n_\chi = s$, and hence $\bar{k} = d$.*

The embeddings that attain the bounds of part 2 (which are, in general, not unique) can be called *maximally pointed* drawings of G .

PROOF. The equality in part (i) comes directly from (14) and (15). For the inequalities, observe that in every pseudo-triangulation we have $d = \bar{k} = 0$ and, hence, $s = n_\chi$. The inequality then follows from the fact that every plane graph can be completed to a pseudo-triangulation with the same number of non-pointed vertices (Theorem 2.5). In the completion process s can only increase, and in the final pseudo-triangulation it equals n_χ .

For part (ii), the only technical part is to show that edges can be added to G to make it rigid but keeping its planarity and its self-stress dimension s . (That is, we want every additional edge to decrease d by one instead of increasing s .)

We prove this claim by induction on d . If $d = 0$ there is nothing to prove. If $d > 0$, let $G(P')$ be any generic plane embedding. Since G is not rigid, there is

an infinitesimal flex in $G(P')$. Some face of the embedding must be deformed by this flex, or otherwise the flex would be trivial. Thus, there is an edge between two vertices of this face that removes one degree of freedom from the space of motions. This edge may produce crossings in the embedding $G(P')$, but since it joins two vertices of a face, the new graph is still planar. This finishes the proof of the claim.

Now, let G_0 be the resulting rigid planar graph with the same s as G . By Theorem 7.1, G_0 can be embedded as a pseudo-triangulation $G_0(P)$, in which $\bar{k} = d = 0$ and hence $n_X = s$. If we remove the additional edges from this embedding to obtain an embedding $G(P)$ of G , the edge removals can certainly not increase n_X . But since s remains constant, any decrease of n_X would violate part (i). Hence $n_X = s$ holds for $G(P)$ as well. \square

8. Polytopes of Pseudo-triangulations

In this section, we describe several high-dimensional polytopes and polyhedra, whose skeletons represent the graphs of certain classes of pseudo-triangulations. We assume familiarity with basic notions of polyhedral theory, such as vertices, faces, or extreme rays. We start with the polyhedral cone of expansive motions of a point set (the *expansion cone*), as defined in the last section. Its extreme rays correspond, in a certain way, to pointed pseudo-triangulations (Theorem 8.1). There are variations of the expansion cone in which the (pointed) pseudo-triangulations are represented more directly: the *pointed pseudo-triangulation polyhedron* and *polytope* (Theorem 8.2), and the *pseudo-triangulation polytope* (Theorem 8.4). Finally, we will mention a polytope corresponding to the pseudotriangulations of a pointgon that lift to locally convex surfaces (Section 4), the *regular pseudo-triangulation polytope* (Theorem 8.6).

8.1. The Expansion Cone. In Section 6, we considered mechanisms which had an expansive infinitesimal motion, i. e., a motion in which all pairwise distances are nondecreasing while certain other distances are held fixed. Abstracting from this mechanism, we may study the space of *all* expansive infinitesimal motions $v = (v_1, \dots, v_n)$ for a point set $P = \{p_1, \dots, p_n\}$. These motions form a polyhedral cone in $(\mathbb{R}^2)^n = \mathbb{R}^{2n}$, given by the $\binom{n}{2}$ homogeneous linear inequalities in the n vector variables $v_i \in \mathbb{R}^2$:

$$(16) \quad \langle p_i - p_j, v_i - v_j \rangle \geq 0, \quad \forall i, j$$

The rigid motions (translations and rotations) of the set P as a whole form a three-dimensional subspace of *trivial motions* for which all inequalities (16) are fulfilled as equations. To get rid of these trivial motions one can arbitrarily pin p_1 by fixing v_1 at 0 (this eliminates the translations) and by restricting the motion of p_2 to the line p_1p_2 (which then eliminates the rotations). Thus we add the following normalizing equations:

$$(17) \quad v_1 = 0, \quad \langle v_2, w \rangle = 0,$$

where w is a vector perpendicular to $p_2 - p_1$. This results in a $(2n - 3)$ -dimensional polyhedral cone, which we call the *expansion cone* $\bar{X}_0 = \bar{X}_0(P)$. The extreme rays of this cone turn out to be exactly the expansive motions defined by the pseudotriangulation mechanisms of Theorem 6.6.

Theorem 8.1. *For a point set P in general position, the expansion cone \bar{X}_0 is a pointed polyhedral cone. Each extreme ray of \bar{X}_0 consists of the expansive infinitesimal motions of a mechanism that is obtained by removing an arbitrary convex hull edge from an arbitrary pointed pseudo-triangulation of P , and each mechanism of this type defines an extreme ray of \bar{X}_0 .*

This theorem will be proved as a consequence of Theorem 8.2 below. Theorem 6.6 about pointed pseudo-triangulation mechanisms is an easy consequence of this theorem, and thus we have another, very indirect, proof for Theorem 6.6, via polytopes.

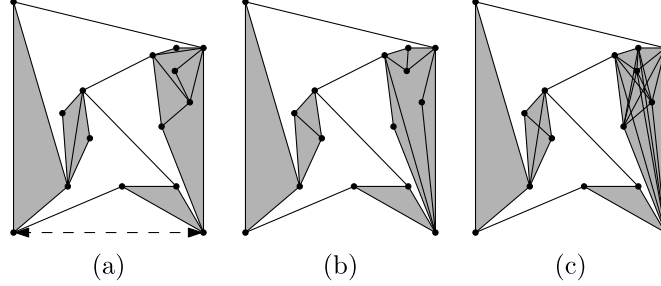


FIGURE 27. (a) A pointed pseudo-triangulation mechanism representing an extreme ray v of the expansion cone. The rigid sub-components are drawn shaded. (b) Another pointed pseudo-triangulation mechanism representing the same extreme ray. (c) The set $E(v)$ of edges whose length is unchanged would be a canonical representation of the ray v .

The correspondence between the extreme rays and the pointed pseudo-triangulations of P is not one-to-one: consider two pseudo-triangulations from which the same convex hull edge has been removed; if they have the same rigid components, they have the same expansive motions and thus they define the same extreme ray, see Figure 27 for an example. (See also Figure 33 in Section 9.5 below.) The rigid components in a pointed pseudo-triangulation mechanism T are formed by the maximal convex regions enclosed by convex cycles in T , and they can be identified in linear time [49].

8.2. The Pointed Pseudo-Triangulation Polyhedron and Polytope.

One can obtain a polyhedron whose vertices are in one-to-one correspondence with the pointed pseudo-triangulations of P by modifying the constraints (16) as follows

$$(16') \quad \langle p_i - p_j, v_i - v_j \rangle \geq f_{ij}, \quad \forall i, j,$$

where the quantities f_{ij} are given by the following squared 2×2 determinants:

$$f_{ij} = |p_i \ p_j|^2$$

The constraints (16') and (17) define a polyhedron $\bar{X}_f = \bar{X}_f(P)$, the *pointed pseudo-triangulation polyhedron*. Moreover, we obtain a bounded polytope by setting some of the equalities (16') to equations

$$(18) \quad \langle p_i - p_j, v_i - v_j \rangle = f_{ij}, \quad \text{for all convex hull edges } ij$$

The resulting polytope, defined by (16'), (17) and (18), is the *pointed pseudo-triangulation polytope* $X_f = X_f$.

Note that, in the sequel, the term *edges* will occur with two meanings: edges of a *polytope*, and edges ij in a geometric *graph* on the point set P . The meaning will always be clear from the context. When we speak about *vertices* in this section, we will always refer to polytope vertices.

For each point $v \in \bar{X}_f$ we may define the index set of tight inequalities:

$$E(v) := \{ ij \mid (16') \text{ holds as an equation for } v \}$$

This set $E(v)$ is taken as the edge set of a geometric graph on P , the support graph of v . By this correspondence, we get precisely the pointed pseudo-triangulations:

Theorem 8.2. *For a set P of n points with n_B points on the convex hull, X_f is a simple polytope of dimension $2n - 3 - n_B$, and \bar{X}_f is a simple polyhedron of dimension $2n - 3$. X_f and \bar{X}_f have the same set of vertices, and they are in one-to-one correspondence with the pointed pseudo-triangulations of P . Two vertices of X_f or \bar{X}_f are adjacent (on the polyhedron), if the corresponding pseudo-triangulations are related by a diagonal flip.*

The extreme rays of \bar{X}_f are in one-to-one correspondence with the pointed pseudo-triangulations of P with one convex-hull edge removed.

In particular, the skeleton of X_f is the graph of pointed pseudo-triangulations defined in Section 2.6.

A consequence of this theorem is that pointed pseudo-triangulations are infinitesimally rigid (Theorem 6.4, for we have given a different proof via the Maxwell-Cremona lifting in Section 6): consider an arbitrary pointed pseudo-triangulation T , and the corresponding vertex v with $E(v) = T$. Since the polytope is simple, the tight inequalities (16') at v must be linearly independent. This means that the corresponding homogeneous system of $2n - 3$ equations

$$\langle p_i - p_j, v_i - v_j \rangle = 0, \quad \forall ij \in E(v)$$

together with (17) has only trivial solutions. In other words, the support graph $E(v)$ is infinitesimally rigid.

The key statement of the proof is the following property of the set of tight edges:

Lemma 8.3. *For a point $v \in \bar{X}_f$, $E(v)$ cannot contain two crossing edges. $E(v)$ cannot contain three edges incident to a common point which make this point non-pointed.*

In particular, $|E(v)| \leq 2n - 3$.

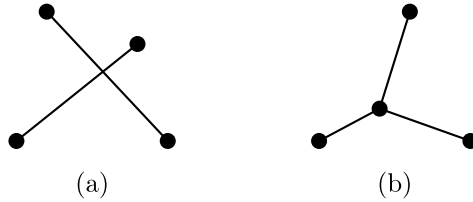


FIGURE 28. (a) Four points in convex position (b) in non-convex position. The shown edges cannot be simultaneously tight.

PROOF. (Sketch.) The statement of the lemma involves only four points: in the first case, they are four points in convex position, and in the second case; a triangle with a fourth point in the middle, see Figure 28. To prove the lemma, one has to show that, for all sets of four points, the inequalities for $ij \in E(v)$ cannot hold as equations while fulfilling the remaining inequalities (16'). This is done by taking an appropriate linear combination of these constraints and deriving a contradiction, which boils down to showing that a certain linear combination of the quantities f_{ij} is positive. It turns out that this linear equation is identically equal to 1.

The bound $|E(v)| \leq 2n - 3$ follows from Theorem 2.6, conditions (4) and (5). \square

Remarkably, both statements of the lemma reduce to the same identity involving the bounds f_{ij} . Rote et al. [45] give a whole family of alternative expressions for f_{ij} that satisfy the same identity and that can be used in (16'). This has only the effect of translating the polyhedra X_f and \bar{X}_f in \mathbb{R}^{2n} , but it does not change their combinatorial properties.

PROOF OF THEOREM 8.2. The proof proceeds now in a somewhat indirect way. First we look at the polyhedron \bar{X}_f . It is easy to see that it has non-empty interior in the $(2n - 3)$ -dimensional subspace defined by (17), and it can be shown that it contains no line. Thus, it has dimension $2n - 3$, and contains at least one vertex v_0 . For every vertex v in a $(2n - 3)$ -dimensional polytope, $E(v)$ must contain at least $2n - 3$ tight edges, but Lemma 8.3 implies that $|E(v)| \leq 2n - 3$. It follows that there are exactly $2n - 3$ tight inequalities, and $E(v)$ is a pointed pseudo-triangulation; hence \bar{X}_f is a simple polyhedron.

The proof that *all* pointed pseudo-triangulations appear as vertices of \bar{X}_f is now somewhat indirect. Every vertex v of the polyhedron is incident to exactly $2n - 3$ polyhedral edges, which lead to adjacent vertices or are infinite extreme rays. Each of these edges is characterized by removing one element from $E(v)$. If this removed element ij is a boundary edge of the convex hull of P , there is no polyhedron vertex v' for which $E(v')$ contains $E(v) - \{ij\}$, and therefore the edge leaving v must be an extreme ray. On the other hand, if the removed element ij is an interior edge of P , there is only one other possible polyhedron vertex v' for which $E(v')$ contains $E(v) - \{ij\}$, namely the pseudo-triangulation $E(v')$ obtained by flipping ij . (One can argue that this polyhedron edge must be a bounded edge, i.e., it is not an extreme ray.)

We have thus proved that for every pointed pseudo-triangulation $E(v)$ represented by a vertex v on the polyhedron, all its neighbors that are obtained by flipping an edge are also represented on \bar{X}_f . Since we know that \bar{X}_f has at least one vertex v_0 , it follows that *all* pointed pseudo-triangulations are represented on \bar{X}_f . Thus, the theorem is proved as far as \bar{X}_f is concerned.

By intersecting \bar{X}_f with the hyperplanes (18), one obtains a face X_f of \bar{X}_f which contains all vertices of \bar{X}_f but none of its extreme rays. Thus, X_f is a bounded polytope that contains the same vertices and (bounded) edges as \bar{X}_f . \square

PROOF OF THEOREM 8.1. \bar{X}_0 is obtained from \bar{X}_f by replacing all right-hand sides f_{ij} by 0, thus \bar{X}_0 is the recession cone of \bar{X}_f . It has a single vertex at the origin, and every extreme ray of \bar{X}_0 comes from one or several extreme rays of \bar{X}_f .

It follows from the definition that every extreme ray of \bar{X}_0 is the expansive motion of a pseudo-triangulation mechanism. \square

8.3. The Pseudo-Triangulation Polytope. One can extend the pointed pseudo-triangulation polytope to a polytope representing *all* pseudo-triangulations, pointed or not, by introducing a variable $t_i \geq 0$ for each point $p_i \in P$, and modifying equations (16') to become

$$(19) \quad \langle p_i - p_j, v_i - v_j \rangle + \|p_i - p_j\| \cdot (t_i + t_j) \geq f_{ij}, \quad \forall i, j,$$

with the same values of f_{ij} , and adding the equations

$$(20) \quad t_i \geq 0, \quad \forall i$$

with equality for boundary vertices. The polytope defined by (20), (19), (17), and (18), is the *pseudo-triangulation polytope* Y_f . By definition, it contains the pointed pseudo-triangulation polytope X_f as the face obtained by setting all the extra variables $t_i = 0$.

Theorem 8.4 ([35]). *For any set P of n points with n_B of them on the convex hull, $Y_f(P)$ is a simple polytope of dimension $3n - 3 - 2n_B$. Its vertices are in one-to-one correspondence with the pseudo-triangulations of P .*

Two vertices of Y_f are adjacent (on the polytope), if the corresponding pseudo-triangulations are related by a (diagonal, insertion, or deletion flip) flip.

Moreover, the faces of the polytope are in one-to-one correspondence with the non-crossing graphs on P . \square

Figure 7 in Section 3 (p. 13) shows the 4-dimensional polytope of all pseudo-triangulations of a certain five-point set, in the form of a Schlegel diagram. More precisely, the solid lines in the figure form the polytope of pointed pseudo-triangulations, of dimension three, which is a wedge of two pentagons. This is a facet of the 4-polytope of all pseudo-triangulations. The other facets appear as a polyhedral subdivision of it into: two tetrahedra, two triangular prisms and two more wedges of two pentagons. These six new facets correspond each to pseudo-triangulations that use one of the six possible interior edges.

Each inequality (19) or (20) defines a facet of Y_f . Setting an inequality (19) to an equation corresponds to insisting that an edge ij is part of the pseudo-triangulation. Setting a variable $t_i = 0$ means that the corresponding vertex has to remain pointed. Thus, each face of Y_f corresponds to a set of *constrained* pseudo-triangulations where certain edges are required to belong to the pseudo-triangulation, and certain vertices are required to be pointed. This has Theorem 2.15 as a corollary.

The pseudo-triangulations of a pointgon (R, P) can also be obtained, indirectly, as a face of $Y_f(P)$: for this, arbitrarily triangulate the exterior of R , and consider the pseudo-triangulations of P constrained to using the boundary of R and this chosen triangulation of the exterior. The vertices of the resulting face are in one-to-one correspondence with the pseudo-triangulations of (R, P) :

Theorem 8.5. *For every pointgon (R, P) there is a simple polytope whose vertices are in one-to-one correspondence with the pseudo-triangulations of (R, P) .* \square

8.4. The Polytope of Regular Pseudo-Triangulations of a Pointgon.

For a pointgon (R, P) one can define another polytope whose vertices represent certain pseudo-triangulations of (R, P) , which are related to locally convex liftings of Section 4.

A *regular* pseudo-triangulation T of a pointgon (R, P) is a pseudo-triangulation of a pointgon (R, P') with $P' \subseteq P$ that can be lifted to a locally convex function on R , in such a way that every interior edge of T is lifted to a strictly convex edge (no two adjacent faces of T are lifted coplanar).

Theorem 8.6 (Aichholzer et al. [5]). *For a pointgon (R, P) , there is a polytope whose vertices are in one-to-one correspondence with the regular pseudo-triangulations of (R, P) .*

Edges on the polytope represent diagonal flips, insertion flips, deletion flips, or vertex removal flips and their converse. \square

The *vertex removal* flips in this statement consist on the deletion of a vertex of degree two and its incident edges. The need for this type of flip comes from the remark we made after Theorem 4.11.

Note that the class of regular pseudo-triangulations is quite different from the set of all pseudo-triangulations of a pointgon, which are represented as a face of $Y_f(P)$, as discussed in Theorem 8.5 at the end of the previous subsection. Firstly, we don't insist that all vertices of P are used in a regular pseudo-triangulation. Secondly, a regular pseudo-triangulation will have no pointed interior vertices, by Lemma 4.2 in Section 4.2.

When R is convex, the regular pseudo-triangulations coincide with the regular triangulations of P . In fact, the proof of the theorem closely follows the construction of the *secondary polytope*, a polytope whose vertices represent the regular triangulations of a point set P [15, 21]. We sketch how this polytope is constructed.

For a given pseudo-triangulation T of (R, P') , specifying a height h_i for every vertex $i \in P$ leads to a unique lifted surface, by the Surface Theorem (Theorem 4.4). This surface depends only on the heights of the complete vertices, and it does so in a linear way. The volume V under the surface (or in other words, the integral of the function whose graph is the surface, over the region R) is therefore a linear function of the heights h_i :

$$V = V_T(h_1, \dots, h_n) = \sum_{i \in P} c_i \cdot h_i$$

The relative pointed vertices and the vertices that are not used at all in T have coefficients $c_i = 0$ in this expression. We use the vector $(c_1, \dots, c_n) \in \mathbb{R}^n$ to represent T . The convex hull of these vectors forms the polytope of Theorem 8.6. Not all vectors will lie on the convex hull of the polytope. It turns out that the vertices of the polytope correspond to the regular pseudo-triangulations.

8.5. Delaunay Pseudo-Triangulations. The Delaunay triangulation of a point set is a very special sample within the family of triangulations, standing out with many remarkable properties. One would wish to have a similar object in the realm of pointed pseudo-triangulations.

Rote and Schulz [46] proposed a definition of a pointed “Delaunay” pseudo-triangulation of a *polygon* R . The definition is based on locally convex liftings of Section 4, but the argument why this is a “reasonable” definition uses the pointed pseudo-triangulation polytope.

For each corner $p_i = (x_i, y_i)$ of R , define $z_i^0 := x_i^2 + y_i^2$, and for each reflex vertex, set z_i^0 to a value larger than all values at the corners. Then the highest locally convex function f below these values will induce a pseudo-triangulation T

of R , by Theorem 4.12. The choice of the values z_i^0 for the reflex vertices ensures that f does not achieve these values, and hence T will be pointed. We call T the pointed Delaunay pseudo-triangulation of R .

To see why this definition might have some justification, let us first consider a convex polygon R . In this case, triangulations and pseudo-triangulations coincide, and one would certainly wish the “Delaunay pseudo-triangulation” to coincide with the Delaunay triangulation. This is indeed the case. However, this coincidence extends to some “neighborhood” of convex polygons: to see this, we have to look at polytopes. For a point set in convex position, the vertices of the secondary polytope [21, 15] represent all triangulations, and a certain canonical objective function c will select the vertex corresponding to the Delaunay triangulation of R . The pointed pseudo-triangulation polytope X_f is an affine image of the secondary polytope, and hence there is an analogous objective function c' , defined from the geometric parameters of R , which selects the Delaunay triangulation on X_f .

Now, we can simply use the same definition of c' for the case when R is not convex. (The secondary polytope and X_f are no longer affinely equivalent; they even have different combinatorial structures.) This objective function picks a vertex of X_f , which represents some pointed pseudo-triangulation T' of the vertex set of R . It can be shown that for a certain class of polygons R , T' contains the boundary of R , and in the interior of R it coincides with the pointed Delaunay pseudo-triangulation T defined above. The precise condition for R is as follows: All corners of R must lie on the convex hull, and any two corners that are separated by just one corner along the boundary can see each other. This class contains non-convex polygons, for which T is a “proper pseudo-triangulation” and not just a triangulation, but it does not contain very “convolved” polygons.

Further properties of these Delaunay pseudo-triangulations have not been investigated so far. Also, there is no satisfactory definition of a “pointed Delaunay pseudo-triangulation of a *point set*”.

9. Applications of Pseudo-Triangulations

9.1. Pseudo-triangulations of Convex Obstacles. In this section, we will briefly review a few problems from the area of motion control and visibility which have been solved with the aid of pseudo-triangulations. In contrast to the previous sections, which dealt with point sets, we will consider a collection of n disjoint convex obstacles in the plane, as mentioned in the introduction, see Fig. 2. For simplicity we assume that the obstacles are smooth and strictly convex, and no three obstacles have a common tangent.

For a line which is tangent to two obstacles, we call the segment between the two points of tangency a *bitangent* if it does not intersect any other obstacle. A *pseudo-triangulation* for a set of convex obstacles is then a maximal set of non-crossing bitangents, see Figure 2. These pseudo-triangulations have analogous properties to pointed pseudo-triangulations of point sets, cf. Theorem 2.6.

Theorem 9.1. (1) *A pseudo-triangulation for a set of n convex obstacles O_1, O_2, \dots, O_n decomposes the free space inside the convex hull, that is, the region*

$$\text{conv}(O_1, O_2, \dots, O_n) - (O_1 \cup O_2 \cup \dots \cup O_n),$$

into pseudo-triangles. In this context, a pseudo-triangle is bounded by three smooth convex curves which meet at three cusps where they have common tangents, such that the convex hull of the cusps contains the pseudo-triangle. The boundary of a pseudo-triangle is a sequence of pieces which strictly alternate between bitangents and pieces of obstacle boundaries.

- (2) A pseudo-triangulation of a set of n convex obstacles has $2n - 2$ pseudo-triangles and $3n - 3$ bitangents. \square

It is straightforward to extend these concepts to obstacles which are not smooth, in particular to polygons. Conceptually, one has to imagine that the polygons are rounded off at the vertices, and the definitions have to be modified accordingly. (In particular, there is a case when two bitangents with a common endpoint are regarded as crossing.)

9.2. The Visibility Complex. The visibility complex is a mathematical structure (a polyhedral complex) and also a data structure that naturally captures visibility in a set of convex obstacles. It was introduced by Pocchiola and Vegter [41]. We consider the set of directed *visibility segments* or *maximal free segments*, which do not intersect any obstacle in the interior, but which cannot be extended without cutting into an obstacle, see Figure 29. Such a segment starts and ends at an obstacle, or it extends to infinity in one or two directions (into the “blue sky”, which, for the purposes of this discussion, can be treated like another obstacle “at infinity”). The segments can be moved continuously, forming a topological space, the *visibility complex*. This space is two-dimensional, as a segment can be locally parameterized by, say, the slope and the signed distance from the origin. All segments which can be transformed into each other while keeping their endpoints on the same two obstacles form a two-dimensional *face* of the visibility complex. A segment reaches the boundary of a face when it becomes tangent to some object. An *edge* of the visibility complex is thus formed by a free segment which is tangent to an object and rotates around this object while keeping its starting point and its terminal point on two other objects. Finally a *vertex* of the visibility complex corresponds to a *bitangent*, a free segment which is simultaneously tangent to two obstacles.

The visibility complex, regarded as a set of vertices, edges, and faces together with the incidences between them, forms an abstract polyhedral complex, which can be stored as a data structure. (A slightly different definition of the visibility complex, which includes additional three-dimensional faces, was given in a successor paper by Pocchiola and Vegter [40].)

Under the general position assumption that no three obstacles share a common tangent, the visibility complex has a quite regular structure: every edge belongs to three faces, and every vertex belongs to four edges and six faces. The face figure of a vertex (formed by these edges and faces) has the combinatorial structure of the graph of a tetrahedron.

The faces of the visibility complex correspond to pseudo-quadrangles where two opposite sides are special: they are formed by a part of a single obstacle boundary or by a convex hull edge.

The set of all bitangents forms the *visibility graph* of the objects, which is a central concept in the context of visibility and shortest path problems. The number k of bitangents of the visibility graph can vary in the range between $\Omega(n)$ and $O(n^2)$.

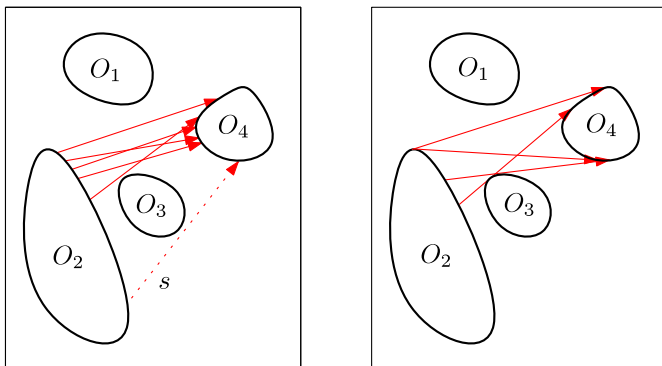


FIGURE 29. A collection of some visibility segments that belong to a common face of the visibility complex. Note that the dotted segment s does not belong to the same face as the other segments although it starts and ends at the same two obstacles O_2 and O_4 . The right part of the figure shows the segments corresponding to the vertices of the face.

The visibility graph itself is not rich enough to allow the computation of the set of visible points from a query point (the visibility region). This is where the additional structure of the visibility complex is helpful. The total complexity of the visibility complex is $\Theta(k)$ if it has k vertices.

Pocchiola and Vegter [41] have shown that the visibility region of a query point can be determined from the visibility complex in $O(m \log n)$ time if its size is m . The algorithm simply sweeps a ray of vision around the query point, and it has to trace a corresponding path through the visibility complex.

Pocchiola and Vegter [40] have given two different algorithms that construct the visibility complex for n obstacles in $O(n \log n + k)$ time with only $O(n)$ intermediate storage, under the assumption that the common tangents between two obstacles can be determined in $O(1)$ time. (Previous algorithms for visibility graphs had achieved the same running time but needed more than linear storage.) The algorithm of [40] uses only simple data structures, but it establishes and exploits a partial order structure on the set of bitangents with strong properties. Roughly speaking, two directed bitangents are related in this partial order when the corresponding free segments can be continuously moved into each other while always maintaining tangency at some obstacle, and changing the direction monotonically. Here the *direction* is measured as an angle in \mathbb{R} , and two directed bitangents which are otherwise the same but whose angle differs by a multiple of 2π are regarded as *different*.

Pseudo-triangulations arise as maximal antichains in this order. The algorithm flips through a sequence of pseudo-triangulations in a simple “greedy” manner and finds all bitangents on the way.

9.3. Geodesic Triangulations. Balanced geodesic triangulations were introduced in [17, 22] as a data structure that performs ray shooting queries and shortest path queries in a dynamically changing connected planar embedded straight-line graph.

Ray shooting refers to the problem of finding the first boundary point that is hit by a query ray. The classical approach to ray shooting, say, in a simple polygon P with n vertices, uses a triangulation of P . After locating the starting point of the query ray in one of the triangles, one follows the ray from triangle to adjacent triangle until the boundary is hit. The running time, after the initial point location step, is proportional to the number of triangles that are transversed, which can be at most $O(n)$, depending on the triangulation. Similarly, a shortest path between two query points can be found quite easily after identifying the unique sequence of triangles which connects the two triangles containing the query points.

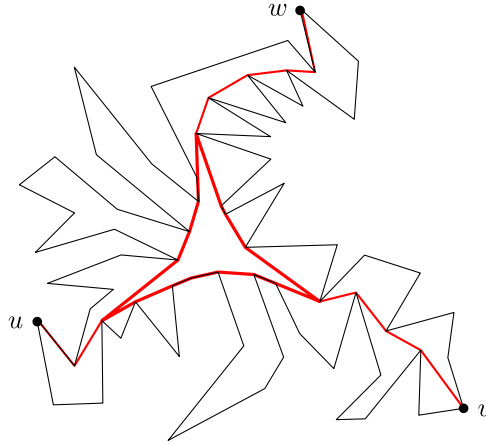


FIGURE 30. A geodesic triangle

We would like to keep the number of triangles on such a path small and at the same time, we want to maintain the search structure under changes of the polygon. For this purpose, we use geodesic triangulations instead of triangulations. Three geodesic paths between uv , vw , and uw will form a *geodesic triangle* which has a pseudo-triangle in the center (which is called a “deltoid region” in [22]) and possibly some complicated paths at each corner which are shared between two geodesic paths, see Figure 30. Let \hat{P} be a convex n -gon whose vertices correspond to the vertices of P as they appear on the boundary. Consider a triangulation \hat{T} of \hat{P} . For every triangle $\hat{u}\hat{v}\hat{w}$ in \hat{T} , we can consider the corresponding geodesic triangle uvw in P . The set of these geodesic triangles will form a *geodesic triangulation* of P , see Figure 31. It is a pseudo-triangulation of the interior of P , but it stores additional information about the correspondence between edges and their original geodesic paths, and about adjacencies in the triangulation \hat{T} . The triangulation \hat{T} of the convex n -gon \hat{P} can be represented as a binary tree (after selecting an edge as the “root”). To follow the above-mentioned paradigm for ray shooting queries, one has to walk through a sequence of geodesic triangles. Going from one geodesic triangle to an adjacent geodesic triangle is no longer a constant-time operation, because geodesic triangles have non-constant size, but it can be carried out in logarithmic time, with appropriated data structures. (A step from a geodesic triangle to an adjacent one may be a zero-length step, in those regions where geodesic triangles have no thickness.)

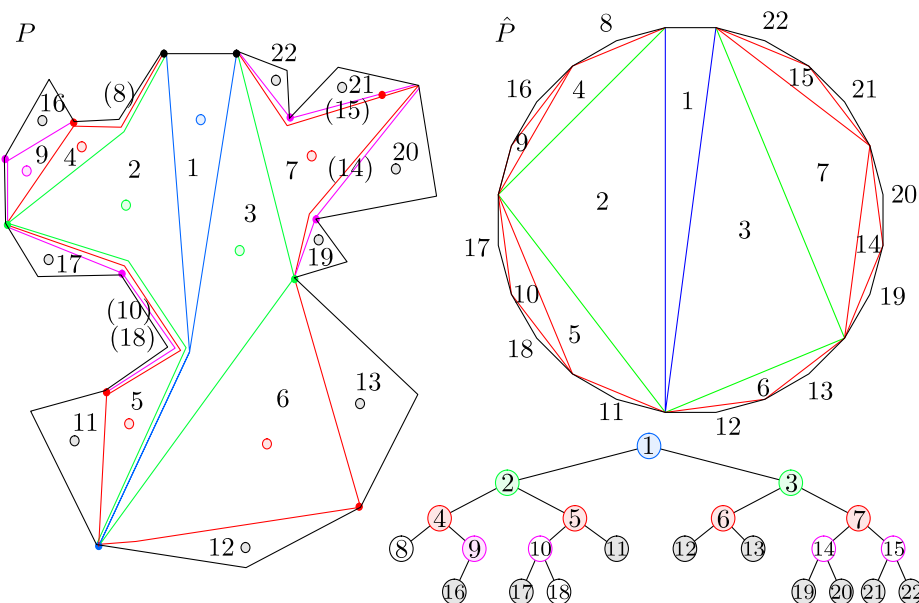


FIGURE 31. A geodesic triangulation of a polygon P , the corresponding triangulation \hat{T} of the convex polygon \hat{P} , and the binary tree representation. Some geodesic triangles in P have no area; their numbers are given in parentheses.

The advantage of using geodesic triangles is that it is easier to get a bound in the number of geodesic triangles traversed. If the triangulation \hat{T} is *balanced* in the sense that it is constructed by always splitting the remaining part of the boundary into roughly equal parts, the number of triangles in any path between two triangles is $O(\log n)$ (which is clearly best possible).

9.4. Kinetic Data Structures for Collision Detection. Pseudo-triangulations were used to maintain a moving set of objects in such a way that collisions can be detected quickly, by Basch et al. [12], Agarwal et al. [1], and Kirkpatrick, Snoeyink, and Speckmann [27, 26, 50]. Consider a set of convex polygons which move simultaneously, under external control or autonomously, together with a pseudo-triangulation of the free space between them, in the sense of Section 9.1. As the points move, the pseudo-triangles will change their shape, but it is easy to check whether it remains a valid pseudo-triangulation:

- Proposition 9.2.** (1) *Consider a pseudo-triangle whose vertices move. It will be a valid pseudo-triangle as long as the following conditions are maintained, see Figure 32:*
- (a) *no two adjacent vertices coincide;*
 - (b) *the three corner angles remain positive;*
 - (c) *all other angles remain larger than π .*
- (2) *Consider a pseudo-triangulation of a set of convex polygons whose vertices move. It will be a valid pseudo-triangulation as long as*
- (a) *all pseudo-triangles remain valid;*
 - (b) *all obstacles remain convex polygons;*

(c) and all exterior angles at the convex hull vertices remain larger than π . \square

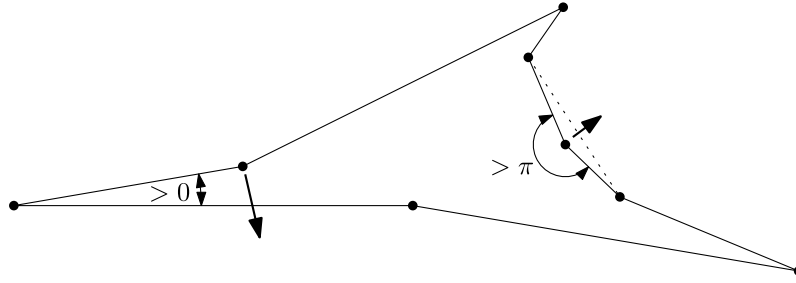


FIGURE 32. Possible violations of the pseudo-triangle condition when vertices move

Thus, when watching the motion of the obstacles, only the conditions of the proposition have to be checked. For example, when the obstacles are rigid or deformable convex polygons, the number of conditions is linear in the number of obstacles and independent of the total number of vertices [27, 50]. When a condition becomes violated, a valid pseudo-triangulation can be restored by a flip.

The approach can be extended to non-convex obstacles, by inserting a pseudo-triangulation into the pockets of the obstacles in a balanced way, as in Section 9.3. With special care about how the maintenance and updates are done, this pseudo-triangulation data structure has good properties in terms of the framework of kinetic data structures. In particular, the overhead in running time is sensitive to the “complexity” of the scene. Objects whose convex hulls are disjoint can be handled faster than interlocked pieces.

A special instance of such a setup, where the pseudo-triangulation is used also to guide the motion, is described in the next section, where it is used to “unfold” a polygon.

9.5. The Carpenter’s Rule Problem. The Carpenter’s Rule Problem asks whether a simple planar polygonal linkage can be continuously reconfigured to any other simple planar configuration with the same edge-lengths, while remaining in the plane and without creating self-intersections along the way. The question was answered in the affirmative by Connelly, Demaine and Rote [19]. The reconfiguring is done by first finding motions that convexify both configurations with expansive motions (which guarantee non-colliding motions), then taking one path in reverse.

We sketch now the subsequent algorithm of Streinu [53], based on pseudo-triangulation mechanisms. The algebraic details of the implementation can be found in [52].

Overview of the Convexification Algorithm. The convexifying path, seen as the collection of the $2n$ trajectories of the $2n$ coordinates $(x_i, y_i), i = 1, \dots, n$ of the vertices of the polygon, is a finite sequence of algebraic curve segments (arcs) connecting continuously at their endpoints.

Each arc corresponds to the unique free motion of the expansive, one-degree-of-freedom mechanism induced by a planar pointed pseudo-triangulation of the given polygon, where a convex hull edge has been removed and another edge has been

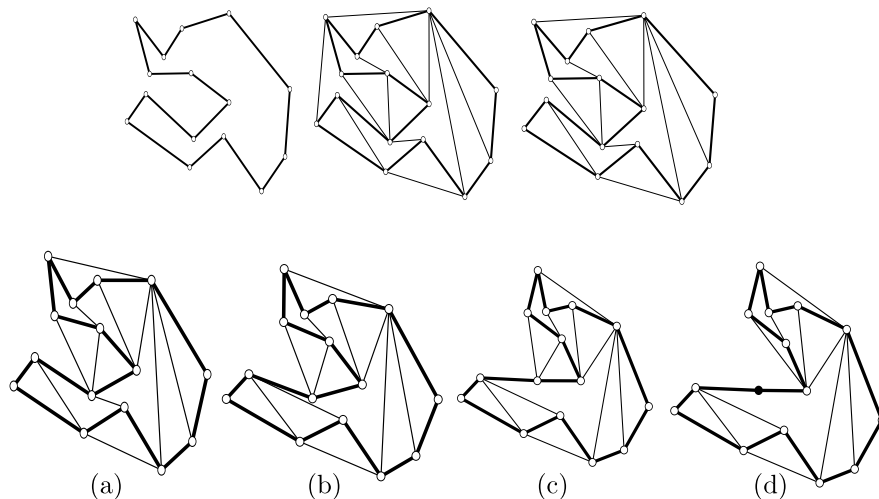


FIGURE 33. Top: A simple polygon, one of its pointed pseudo-triangulations and a pseudo-triangulation mechanism obtained by removing a convex hull edge. Bottom: (a) The mechanism just before an alignment event and (b) after the event, when a flip was performed. (c) Continuing the motion, the next event aligns two polygon edges. (d) The aligned vertex (black) is frozen, the pseudo-triangulation is locally restructured and the motion can continue.

pinned down. The mechanism is constructed by adding $n - 4$ bars to the original polygon in such a way that there are no crossings, each vertex is incident to an angle larger than π and exactly one convex hull edge is missing. See Fig. 33. This can be done algorithmically in $O(n)$ time. The mechanism is then set in motion by pinning down one edge and rotating another edge around one of its joints. The framework now moves *expansively*, thus guaranteeing a collision-free trajectory. One step of the convexification algorithm consists in moving this mechanism until two incident edges align (see Figure 32). At this moment it ceases to be a pointed pseudo-triangulation. We either freeze a joint (if the aligned edges belong to the polygon) and locally patch a pointed pseudo-triangulation for a polygon with one less vertex, or otherwise perform a local flip of the added diagonals. See Fig. 33.

Algorithm 9.3. (The Pseudo-Triangulation Road-Map Algorithm)

- (1) **Initialization:** Pseudo-triangulate the polygon. Remove a convex hull edge to obtain a pseudo-triangulation expansive mechanism.
- (2) **Repeat until the polygon becomes convex:**
 - **(Next Event)** Move the mechanism until an *alignment event* occurs: two extreme edges at a vertex align.
 - **(Freeze or Flip)** If the aligned edges were polygon edges, *freeze* them into a single edge by eliminating the common vertex, and recompute a compatible pseudo-triangulation mechanism. If one of the aligned edges is an added edge, drop it and replace it by the edge extending over the two aligned edges (see Fig. 33(a-b)).

There are many ways to construct the initial pointed pseudo-triangulation or to readjust it at an alignment event. For the sake of the analysis, [53] uses a canonical pseudo-triangulation based on shortest-path trees inside the polygon and its pockets. This helps us maintain a global integer valued cost function, the total number of bends in the shortest paths, which is bounded by $O(n^2)$ for n active (not frozen) vertices. The cost function decreases by at least one at flip-alignment events and increases at most $n - 3$ times, at freeze events. This analysis bounds the total number of events, and thus the number of steps induced by simple pseudo-triangulation mechanism motions, by $O(n^3)$.

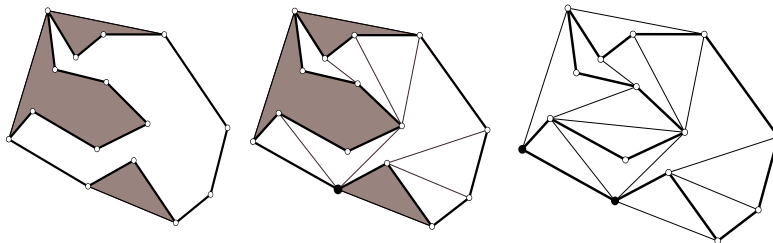


FIGURE 34. Left: The pockets of the polygon from Fig. 33. Middle: the shortest-path-tree pseudo-triangulation of the interior of the polygon. The source vertex of the tree is black. Right: a complete pointed pseudo-triangulation obtained by taking shortest path trees in all the pockets, and in the interior of the polygon.

9.6. Spherical Pseudo-Triangulations and Single-Vertex Origami. An *origami* is a piece of paper with creases, which is meant to be folded into a three dimensional shape without bending or stretching the paper (just folding along the creases). A very special case, the *single-vertex origami* illustrated in Figure 35, turns out to be nothing but the Carpenter’s Rule Problem in spherical geometry, see Streinu and Whiteley [55].

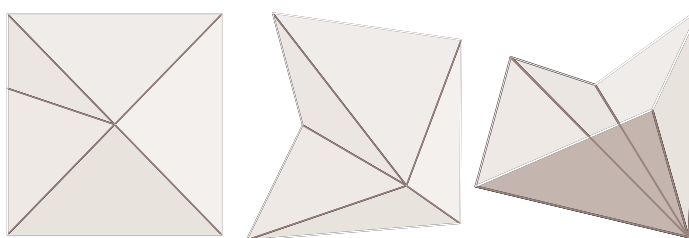


FIGURE 35. A single-vertex origami fold: (a) the creased piece of paper; (b,c) two of its possible folded states.

The idea is to associate to every planar framework, via central projection, a framework on the sphere, with vertices placed as points on a sphere and with edges along great-circles. This connection is illustrated in Figure 36. Furthermore, by connecting the vertices with the center of the sphere, we obtain a series of triangles (which behave in 3-space like rigid panels) connected along hinges into a conical

structure, as in Figure 36. This simple sequence of transformations transforms planar pseudo-triangulations into spherical or conical structures which inherit all the expansiveness properties of the planar ones.

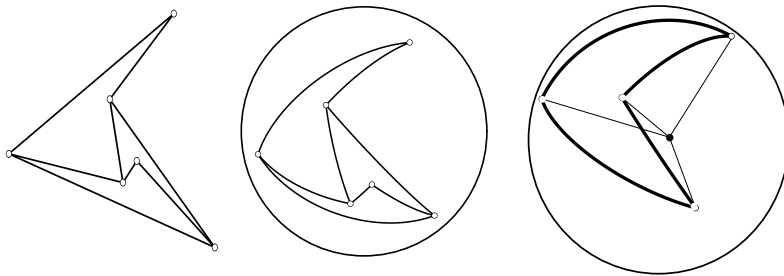


FIGURE 36. A planar pseudo-triangulation, its corresponding spherical version, and a conical panel-and-hinge structure arising from a (different) pseudo-triangulation.

By translating all relevant concepts of the pseudo-triangulation road-map algorithm for the planar Carpenter's Rule problem, one obtains:

Theorem 9.4 (Streinu and Whiteley [55]). *Every simple spherical polygon with perimeter at most 2π can be convexified in a hemisphere. Every single vertex origami can be folded from a flat piece of paper.*

9.7. Spherical Pseudo-Triangulations and Convex Geometry. We mentioned in the introduction that a pseudo-triangulation in the plane can have at most one pseudo- k -gon with $k < 3$, namely the outer face. This property remains true for pseudo-triangulations on the sphere that are restricted to lie in a hemisphere, such as the ones that arise in the previous subsection. However, if we look at pseudo-triangulations on the whole sphere, it turns out that one can have an arbitrary number of pseudo-2-gons. Therefore, the bound of $2n - 3$ on the number of edges of pointed graphs, which follows from Theorem 2.9, does not hold; pointed graphs with $2n - 2$ or more edges exist. As graphs in the sphere these graphs support a self-stress and have therefore a piecewise linear lifting (in an appropriate sense). Panina [37] has used these liftings to construct counter-examples to a conjecture of A. D. Alexandrov about a characterization of the sphere among the smooth convex surfaces. The crucial property, which follows from pointedness, is that the liftings are *saddle functions*, in a sense analogous to the properties of pointed vertices p in the liftings of pseudotriangulations with a unique non-pointed vertex, which were mentioned at the end of Section 5.2: at the lifted point p' , there is no supporting plane which intersects the neighborhood of the lifted surface f only in this point (and leaves the surface locally on one side of it). See Panina [38] for more information on the connections between pseudo-triangulations, saddle function, and so-called hyperbolic virtual polytopes.

9.8. Guarding Polygons with π -Guards. *Art Galleries* and *Illumination* are a popular category of geometric problems, where one asks for the number of *guards*, placed in the interior of a planar region so that they would entirely cover it, or for light sources that would illuminate it entirely. Bounds on the necessary number of guards have been traditionally obtained using decompositions into convex

regions, in particular triangles, which can be covered with exactly one guard placed at any vertex. Speckmann and Tóth [51] improved the known bounds for guarding a polygon with *restricted visibility* guards by employing pseudo-triangulations. A π -guard is a placement of a π angle at a vertex of the polygon.

Theorem 9.5 (Speckmann and Tóth [51]). *Any simple polygon with n vertices, k of which are convex, can be monitored with $\lfloor \frac{2n-k}{3} \rfloor$ edge-aligned π -guards.* \square

9.9. Pseudo-Triangulations and Pseudoline Arrangements. The term *pseudo-triangulation* was coined by Pocchiola and Vegter [39] because of an interesting connection with pseudoline arrangements. We conclude our list of applications with their intriguing observation.

Pseudoline arrangements. A *pseudoline* is a simple planar curve which partitions the Euclidean plane into two parts. A *pseudoline arrangement* is a collection of pseudolines, each pair of which has exactly one crossing.

Tangents to pseudo-triangles. For any given direction, a pseudo-triangle has a unique tangent parallel to this direction, in the sense defined in Section 2.2 before Lemma 2.3 (p. 7). Two disjoint pseudo-triangles have exactly one common tangent, see Fig. 37.

Duality: from pseudo-triangles to pseudoline arrangements. If we dualize the lines carrying the tangents of a pseudo-triangle (using the standard concept of point-line duality in the Euclidean plane), we obtain an x -monotone curve. The unique tangent property implies that the duals of a collection of pseudo-triangles with disjoint interiors form indeed a pseudoline arrangement.

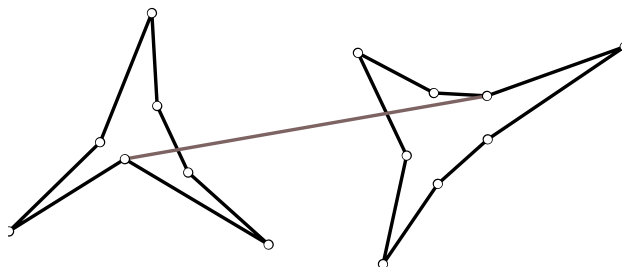


FIGURE 37. Two pseudo-triangles and their unique common tangent.

References

- [1] P. Agarwal, J. Basch, L. Guibas, J. Hershberger, and L. Zhang. Deformable free space tilings for kinetic collision detection. *International Journal of Robotics Research*, 21:179–197, 2003.
- [2] O. Aichholzer, F. Aurenhammer, and T. Hackl. Pre-triangulations and liftable complexes. In N. Amenta and O. Cheong, editors, *Proceedings 22nd Ann. Symp. Comput. Geom., Sedona, Arizona, USA, June 5–7, 2006*, pages 282–291. ACM, 2006.
- [3] O. Aichholzer, F. Aurenhammer, C. Huemer, and H. Krasser. Transforming spanning trees and pseudo-triangulations. *Inf. Process. Lett.*, 97(1):19–22, 2006.
- [4] O. Aichholzer, F. Aurenhammer, and H. Krasser. Adapting (pseudo)-triangulations with a near-linear number of edge flips. In *Proc. 8th International Workshop on Algorithms and Data Structures (WADS)*, volume 2748 of *Lecture Notes in Computer Science*, pages 12–24, 2003.
- [5] O. Aichholzer, F. Aurenhammer, H. Krasser, and P. Brass. Pseudo-triangulations from surfaces and a novel type of edge flip. *SIAM Journal on Computing*, 32:1621–1653, 2003.

- [6] O. Aichholzer, F. Aurenhammer, H. Krasser, and B. Speckmann. Convexity minimizes pseudo-triangulations. *Computational Geometry: Theory and Applications*, 28:3–10, 2004.
- [7] O. Aichholzer, M. Hoffmann, B. Speckmann, and C. D. Tóth. Degree bounds for constrained pseudo-triangulations. In *Proc. 15th Canadian Conference on Computational Geometry (CCCG 2003)*, pages 155–158, Halifax, Nova Scotia, Canada, 2003.
- [8] O. Aichholzer, F. Hurtado, and M. Noy. A lower bound on the number of triangulations of planar point sets. *Computational Geometry: Theory and Applications*, 29:135–145, 2004.
- [9] O. Aichholzer, D. Orden, F. Santos, and B. Speckmann. On the number of pseudo-triangulations of certain point sets. *J. Combin. Theory Ser. A*, 2007. To appear.
- [10] O. Aichholzer, G. Rote, B. Speckmann, and I. Streinu. The zig-zag path of a pseudo-triangulation. In *Proc. 8th International Workshop on Algorithms and Data Structures (WADS)*, volume 2748 of *Lecture Notes in Computer Science*, pages 377–388, Ottawa, Canada, 2003. Springer-Verlag.
- [11] D. Avis and K. Fukuda. Reverse search for enumeration. *Discrete Applied Mathematics*, 65(1-3):21–46, 1996.
- [12] J. Basch, J. Erickson, L. Guibas, J. Hershberger, and L. Zhang. Kinetic collision detection for two simple polygons. *Computational Geometry: Theory and Applications*, 27:211–235, 2004.
- [13] S. Bereg. Transforming pseudo-triangulations. *Information Processing Letters*, 90(3):141–145, 2004.
- [14] S. Bereg. Enumerating pseudo-triangulations in the plane. *Comput. Geom. Theory Appl.*, 30(3):207–222, 2005.
- [15] L. Billera, P. Filliman, and B. Sturmfels. Constructions and complexity of secondary polytopes. *Advances in Mathematics*, 83:155–179, 1990.
- [16] H. Brönnimann, L. Kettner, M. Pocchiola, and J. Snoeyink. Counting and enumerating pointed pseudotriangulations with the greedy flip algorithm. *SIAM Journal on Computing*, 36:721–739, 2006.
- [17] B. Chazelle, H. Edelsbrunner, M. Grigni, L. J. Guibas, J. Hershberger, M. Sharir, and J. Snoeyink. Ray shooting in polygons using geodesic triangulations. *Algorithmica*, 12:54–68, 1994.
- [18] É. Colin de Verdière, M. Pocchiola, and G. Vegter. Tutte’s barycenter method applied to isotopies. *Computational Geometry: Theory and Applications*, 26(1):81–97, 2003.
- [19] R. Connelly, E. Demaine, and G. Rote. Straightening polygonal arcs and convexifying polygonal cycles. *Discrete and Computational Geometry*, 30(2):205–239, August 2003.
- [20] H. Edelsbrunner and N. R. Shah. Incremental topological flipping works for regular triangulations. *Algorithmica*, 15:223–241, 1996.
- [21] I. M. Gel’fand, M. M. Kapranov, and A. V. Zelevinsky. *Discriminants, Resultants and Multidimensional Determinants*. Birkhäuser, Boston, 1994.
- [22] M. T. Goodrich and R. Tamassia. Dynamic ray shooting and shortest paths in planar subdivisions via balanced geodesic triangulations. *Journal of Algorithms*, 23:51–73, 1997.
- [23] J. Graver, B. Servatius, and H. Servatius. *Combinatorial Rigidity*. Graduate Studies in Mathematics vol. 2. American Mathematical Society, 1993.
- [24] R. Haas, D. Orden, G. Rote, F. Santos, B. Servatius, H. Servatius, D. Souvaine, I. Streinu, and W. Whiteley. Planar minimally rigid graphs and pseudo-triangulations. *Computational Geometry: Theory and Applications*, 31:31–61, 2005.
- [25] L. Kettner, D. Kirkpatrick, A. Mantler, J. Snoeyink, B. Speckmann, and F. Takeuchi. Tight degree bounds for pseudo-triangulations of points. *Computational Geometry: Theory and Applications*, 25:3–12, 2003.
- [26] D. Kirkpatrick, J. Snoeyink, and B. Speckmann. Kinetic collision detection for simple polygons. *International Journal of Computational Geometry and Applications*, 12:3–27, 2002.
- [27] D. Kirkpatrick and B. Speckmann. Kinetic maintenance of context-sensitive hierarchical representations for disjoint simple polygons. In *Proc. 18th Ann. Symposium on Computational Geometry (SoCG)*, pages 179–188, 2002.
- [28] G. Laman. On graphs and rigidity of plane skeletal structures. *Journal of Engineering Mathematics*, 4:331–340, 1970.
- [29] C. Lee. The associahedron and triangulations of the n -gon. *European Journal of Combinatorics*, 10:551–560, 1989.
- [30] J. C. Maxwell. On reciprocal figures and diagrams of forces. *Philosophical Magazine*, 27:250–261, 1864.

- [31] J. C. Maxwell. On reciprocal figures, frames and diagrams of forces. *Transactions of the Royal Society Edinburgh*, 26:1–40, 1870.
- [32] J. C. Maxwell. On Bow’s method of drawing diagrams in graphical statics, with illustrations from Peaucellier’s linkage. *Cambridge Phil. Soc. Proc.*, 2:407–414, 1876.
- [33] P. McCabe and R. Seidel. New lower bounds for the number of straight-edge triangulations of a planar point set. In *Abstracts of the 20th European Workshop on Computational Geometry*, pages 175–176, Seville, Spain, Mar. 2004.
- [34] D. Orden, G. Rote, F. Santos, B. Servatius, H. Servatius, and W. Whiteley. Non-crossing frameworks with non-crossing reciprocals. *Discrete and Computational Geometry*, 32:567–600, 2004.
- [35] D. Orden and F. Santos. The polytope of non-crossing graphs on a planar point set. *Discrete and Computational Geometry*, 32:275–305, 2005.
- [36] D. Orden, F. Santos, B. Servatius, and H. Servatius. Combinatorial pseudo-triangulations. *Discrete Mathematics*, 2007. To appear.
- [37] G. Panina. New counterexamples to A. D. Alexandrov’s hypothesis. *Adv. Geom.*, 5(2):301–317, 2005.
- [38] G. Panina. Planar pseudo-triangulations, spherical pseudo-tilings and hyperbolic virtual polytopes. Technical Report math.MG:0607171, arXiv, 2006.
- [39] M. Pocchiola and G. Vegter. Order types and visibility types of configurations of disjoint convex plane sets. Technical Report LIENS, January 1994.
- [40] M. Pocchiola and G. Vegter. Topologically sweeping visibility complexes via pseudo-triangulations. *Discrete & Computational Geometry*, 16(4):419–453, 1996.
- [41] M. Pocchiola and G. Vegter. The visibility complex. *International Journal of Computational Geometry and Applications*, 6(13):279–308, 1996.
- [42] D. Randall, G. Rote, F. Santos, and J. Snoeyink. Counting triangulations and pseudo-triangulations of wheels. In *Proc. 13th Canadian Conf. Computational Geometry, Waterloo*, pages 149–152, 2001.
- [43] A. Récski. *Matroid Theory and its Applications*. Springer-Verlag, 1989.
- [44] J. Richter-Gebert. *Realization Spaces of Polytopes*. Springer-Verlag, 1996.
- [45] G. Rote, F. Santos, and I. Streinu. Expansive motions and the polytope of pointed pseudo-triangulations. In B. Aronov, S. Basu, J. Pach, and M. Sharir, editors, *Discrete and Computational Geometry – The Goodman-Pollack Festschrift*, pages 699–736. Springer-Verlag, Berlin, 2003.
- [46] G. Rote and A. Schulz. A pointed Delaunay pseudo-triangulation of a simple polygon. In *Abstracts of the 21st European Workshop on Computational Geometry*, pages 77–80, Eindhoven, Mar. 2005.
- [47] G. Rote, C. A. Wang, L. Wang, and Y. Xu. On constrained minimum pseudo-triangulations. In T. Warnow and B. Zhu, editors, *Computing and Combinatorics, Proc. 9th Ann. Intern. Computing and Combinatorics Conf. (COCOON 2003)*, volume 2697 of *Lecture Notes in Computer Science*, pages 445–454, Big Sky, USA, July 2003. Springer-Verlag.
- [48] M. Sharir and E. Welzl. Random triangulations of planar point sets. In *Proc. 22nd Ann. Symp. Comput. Geom. (SoCG)*, pages 273–281. ACM, 2006.
- [49] J. Snoeyink and I. Streinu. Computing rigid components of pseudo-triangulation mechanisms in linear time. In *Proc. 17th Canadian Conference on Computational Geometry (CCCG 2005)*, pages 223–226, Windsor, Ontario, Canada, 2005.
- [50] B. Speckmann. *Kinetic Data Structures for Collision Detection*. PhD thesis, Dept. of Computer Science, University of British Columbia, 2001.
- [51] B. Speckmann and C. D. Tóth. Allocating vertex π -guards in simple polygons via pseudo-triangulations. *Discrete and Computational Geometry*, 33:345–364, 2005.
- [52] I. Streinu. Combinatorial roadmaps in configuration spaces of simple planar polygons. In S. Basu and L. González-Vega, editors, *DIMACS Workshop on Algorithmic and Quantitative Aspects of Real Algebraic Geometry in Mathematics and Computer Science, March 12–16, 2001, DIMACS Center, Rutgers University, Piscataway, NJ, USA*, pages 181–206. American Mathematical Society, 2001.
- [53] I. Streinu. Pseudo-triangulations, rigidity and motion planning. *Discrete and Computational Geometry*, 34:587–635, December 2005.
- [54] I. Streinu. Parallel redrawing mechanisms, pseudo-triangulations and kinetic planar graphs. In P. Healy and N. S. Nikolov, editors, *Proc. 13th International Symposium on Graph Drawing*

- (GD 2005), Limerick, Ireland, September 12–14, 2005, *Revised Papers*, volume 3843 of *Lecture Notes in Computer Science*, pages 421–433, 2006.
- [55] I. Streinu and W. Whiteley. Single-vertex origami and spherical expansive motions. In J. Akiyama and M. Kano, editors, *Proc. Japan Conf. Discrete and Computational Geometry (JCDCG 2004)*, volume 3742 of *Lecture Notes in Computer Science*, pages 161–173, Tokai University, Tokyo, 8–11 October 2004 2005. Springer-Verlag.
- [56] W. Whiteley. Some matroids from discrete applied geometry. In J. O. J. Bonin and B. Servatius, editors, *Matroid Theory*, volume 197 of *Contemporary Mathematics*, pages 171–311. American Mathematical Society, 1996.
- [57] W. Whiteley. Rigidity and scene analysis. In J. E. Goodman and J. O'Rourke, editors, *Handbook of Discrete and Computational Geometry*, chapter 60, pages 1327–1354. CRC Press, Boca Raton New York, second edition, 2004.

INSTITUT FÜR INFORMATIK, FREIE UNIVERSITÄT BERLIN, TAKUSTRASSE 9, D-14195 BERLIN, GERMANY.

E-mail address: `rote@inf.fu-berlin.de`

DEPARTAMENTO DE MATEMÁTICAS, ESTADÍSTICA Y COMPUTACIÓN, UNIVERSIDAD DE CANTABRIA, E-39005 SANTANDER, SPAIN

E-mail address: `francisco.santos@unican.es`

DEPARTMENT OF COMPUTER SCIENCE, SMITH COLLEGE, NORTHAMPTON, MA 01063, USA.

E-mail address: `streinu@cs.smith.edu`